Tenuivirus uses a molecular bridge strategy to overcome insect midgut barriers for virus persistent transmission

Gang Lu[1], Shuo Li[2], Changwei Zhou[1], Xin Qian[1], Qing Xiang[1], Tongqing Yang[1], Jianxiang Wu[3], Xueping Zhou[3,4], Yijun Zhou[2*], Xin Shun Ding[1] and Xiaorong Tao[1*]

[1] Department of Plant Pathology, Nanjing Agricultural University, Nanjing 210095, P.R. China

[2] Institute of Plant Protection, Jiangsu Academy of Agricultural Sciences, Jiangsu Technical Service Center of Diagnosis and Detection for Plant Virus Diseases, Nanjing 210014, P.R. China

[3] State Key Laboratory of Rice Biology, Institute of Biotechnology, Zhejiang University, Hangzhou 310029, P.R. China

[4] State Key Laboratory for Biology of Plant Diseases and Insect Pests, Institute of Plant Protection, Chinese Academy of Agricultural Sciences, Beijing 100193, P.R. China

[*]To whom correspondence should be addressed. Email: taoxiaorong@njau.edu.cn (X.T.) or yjzhou@jass.ac.cn (Y.Z.).

Running title

A molecular bridge model for virus persistent transmission

Abstract

Many persistent transmitted plant viruses, including *Rice stripe tenuivirus* (RSV), cause serious damages to crop productions in China and worldwide. Although many reports have indicated that successful insect-mediated virus transmission depends on proper virus–insect vector interactions, the mechanism(s) controlling interactions between viruses and insect vectors for virus persistent transmission remained poorly understood. In this study, we used RSV and its small brown planthopper (SBPH) vector as a working model to elucidate the molecular mechanism controlling RSV virion entrance into SBPH midgut for persistent transmission. We have now demonstrated that this non-enveloped *Tenuivirus* uses its non-structural glycoprotein NSvc2 as a helper component to bridge the specific interaction between virion and SBPH midgut cells, leading to overcome SBPH midgut barriers for virus persistent transmission. In the absence of this glycoprotein, purified RSV virion is not capable of entering SBPH midgut cells. In RSV-infected cells, glycoprotein NSvc2 is processed into two mature proteins: an amino-terminal protein NSvc2-N and a carboxyl-terminal protein NSvc2-C. We determined that NSvc2-N interacted with RSV virion and bound directly to midgut lumen surface via its N-glycosylation sites. Upon recognition by midgut cells, the midgut cells underwent endocytosis followed by compartmentalizing RSV virion and NSvc2 into early and then late endosomes. The acidic condition inside the late endosome triggered conformation change of NSvc2-C and caused cell membrane fusion via its highly conserved fusion loop motifs, leading to the release of RSV virion from endosome into cytosol. In summary,

42 our results showed for the first time that a rice *Tenuivirus* uses a molecular bridge
43 strategy to ensure proper interactions between virus and insect midgut for successful
44 persistent transmission.
45

46 ## Author summary

47 Over 75% of the known plant viruses are insect transmitted. Understanding how plant
48 viruses interacted with their insect vectors during virus transmission is one of the key
49 steps to manage virus diseases worldwide. Both the direct and indirect virus–insect
50 vector interaction models have been proposed for virus non-persistent and
51 semi-persistent transmission. However, the indirect virus–vector interaction
52 mechanism during virus persistent transmission has not been reported previously. In
53 this study, we developed a new reverse genetics technology and demonstrated that the
54 circulative and propagative transmitted *Rice stripe tenuivirus* utilizes a glycoprotein
55 NSvc2 as a helper component to ensure a specific interaction between *Tenuivirus*
56 virion and midgut cells of small brown planthopper (SBPH), leading to conquering
57 the midgut barrier of SBPH. This is the first report of a helper component
58 mediated-molecular bridge mechanism for virus persistent transmission. These new
59 findings and our new model on persistent transmission expand our understanding of
60 molecular mechanism(s) controlling virus–insect vector interactions during virus
61 transmission in nature.
62

63

Introduction

Arthropod insects play critical roles in epidemics of numerous animal and plant viruses [1-3]. Based on the mode of transmission, plant viruses can be classified into non-persistent, semi-persistent or persistent transmitted viruses [4-6]. For non-persistent and semi-persistent transmissions, plant viruses retain only inside insect stylets or on foregut surface for a short period of time. Upon probing or feeding on a new host plant, viruses are quickly injected into plant cells, together with insect saliva [7-9]. The persistent transmitted plant viruses (non-propagative or propagative) are required to enter insect vector bodies, and then circulate and/or replicate inside the vectors for several days to weeks. These persistent transmitted viruses need to pass insect midgut barrier, dissemination barrier, and then salivary gland barrier prior to be transmitted to new host plants [6, 10, 11]. Midgut is often considered to be one of major barriers for successful persistent transmissions of plant viruses. During the process of passing through barriers inside vectors, proper interactions between viruses and vectors are needed for successful transmission. However, the mechanism controlling the interactions between persistent transmitted plant viruses and their insect vector midgut barriers remains poorly understood.

Molecular bridge mechanism has been reported for non-persistent and semi-persistent transmitted plant viruses, respectively [4, 12, 13]. For example, virion of non-persistent or semi-persistent transmitted plant viruses were reported to interact with the cuticular proteins in the mouthparts or the foreguts [14, 15], and these

virus–insect interactions required virally encoded non-structural helper factors as molecular bridges [12, 13]. Viruses in the genus *Potyvirus* are known to encode a helper component proteinase (HC-Pro) and this HC-Pro protein acts as a molecular bridge for potyvirus virion–aphid vector interactions [16-18]. Members in the genus *Caulimovirus* encode a different helper factor that helps virion to retain on insect maxillary stylet [19-21]. Although virion of multiple persistent transmitted plant viruses [e.g., *Luteovirus* [22, 23], *Geminivirus* [24, 25], *Reovirus* [26, 27], *Tospovirus* [28, 29], and plant *Rhabdovirus* [30, 31]] were also reported to bind directly to insect midgut cells, these bindings all depended on virion surface-exposed proteins. To date, no persistent transmitted (non-propagative or propagative) plants viruses has been reported for the requirement of additional helper proteins for the transmission.

Rice stripe tenuivirus (RSV) is known to be transmitted by small brown planthopper (SBPH) in a circulative and propagative manner, and causes severe rice losses in China and many other countries in Asia [32, 33]. The genome sequence of plant infecting *Tenuivirus* is similar to members of animal infecting *Phlebovirus* in the order of *Bunyavirales.* Most of the members in the order of *Bunyavirales* produce membrane-enveloped spherical virion with two surface-exposed glycoproteins. These surface-exposed glycoproteins are key determinants for entering host cells or for vector transmission [29, 34, 35]. However, virion of tenuiviruses are filamentous and do not have enveloped membranes. Purified tenuivirus virion was previously reported to be non-transmissible by vector insects [36-38]. RSV also encodes a glycoprotein NSvc2, which can be further processed into an amino-terminal part protein known as

NSvc2-N and a carboxyl-terminal part protein known as NSvc2-C [39, 40]. The RSV encoded glycoprotein NSvc2 was not found in the purified virion samples [41, 42]. Based on the above published reports we hypothesized that *Rice stripe tenuivirus* must use a quite different mechanism to overcome the midgut barriers for its insect transmission.

To validate this hypothesis, we conducted various experiments using RSV and SBPH as our working model. We have now determined for the first time that the rice *Tenuivirus* uses a unique molecular bridge strategy to overcome insect midgut barrier for virus persistent transmission. We have shown that in the absence of RSV non-structural glycoprotein NSvc2, RSV virion was unable to enter SBPH midgut cells. We found that this RSV non-structural glycoprotein NSvc2 acts as a critical molecular bridge to mediate the interaction between RSV virion and SBPH midgut. NSvc2-N, a processed product from NSvc2, interacts with RSV virion and binds directly to the midgut barrier. Upon the successful interaction, midgut cells undergo endocytosis followed by compartmentalization of RSV virion and NSvc2 complexes in early and then late endosomes. NSvc2-C, another processed product from NSvc2, triggers membrane fusion under the acidic condition inside the late endosomes to release RSV virion into cytosol. These new findings expand our understanding of interactions between virion and insect vectors during transmissions of plant and animal viruses.

Results

Association of NSvc2 protein with RSV virion in midgut of SBPH

To examine whether RSV NSvc2 plays role(s) in circulative RSV transmission, we first conducted a time course study on the co-localization of NSvc2 and RSV virion in the midgut of SBPH during acquisition. SBPHs were fed on RSV-infected rice seedlings and then collected at 4, 8, 16 and 24 h after feeding (30 SBPHs at each time point), respectively. The collected insects were dissected and analyzed for the presence of NSvc2 and RSV virion by double-immunolabeling methods using an antibody against the amino-terminal NSvc2 (NSvc2-N) or RSV virion-surface nucleocapsid protein (NP). As shown in Fig 1A that, after 4 h feeding on the RSV-infected rice seedlings, numerous RSV virion (green) had accumulated in the midgut lumen. In the same tissues, NSvc2 was also detected (red) and found to co-localize with RSV virion on the actin-labelled intestinal microvillus (blue) (Fig 1A). The overlapped coefficient (OC) value for the red and green labeling signal was 0.76 ± 0.03 at 4 h post feeding (Fig 1E), indicating that NSvc2 and RSV virion were localized close to each other. At 8 h post feeding, NSvc2 was found to co-localize with RSV virion in various sized vesicles-like structures in epithelial cells (Fig 1B). Analysis of OC value showed again that NSvc2 and RSV were indeed localized close to each other (Fig 1F). At 16 h post feeding, RSV virion was detected together with NSvc2 in cytoplasm of midgut epithelial cells, with an OC value of 0.73 ± 0.06 (Fig 1C and 1G). Even at 24 h post feeding, NSvc2 was still associated with RSV virion, with an OC value of 0.76 ± 0.04, and the virus had spread into the surrounding midgut epithelial cells (Fig 1D and 1H). These data showed that RSV-encoded glycoprotein

NSvc2 was associated with RSV virion in SBPH midgut during insect feeding on RSV-infected rice plants.

NSvc2 protein is critical for RSV virion entrance into SBPH midgut

RSV virion was purified from virus-infected rice seedlings through ultracentrifugation using a 20% glycerol cushion. After ultracentrifugation, four different fractions starting from the top of the upper supernatant phase (Sup1 to Sup4), four fractions starting from the top of the lower 20 % glycerol phase (Gly1 to Gly4), and the pellet (Pel) were collected and analyzed individually by immunoblotting assays using an antibody against RSV NP or NSvc2-N (Fig 2A and 2B). Results showed that the pellet sample contained RSV virion, and the four supernatant fractions (Sup1 to Sup4) contained NSvc2 protein. In contrast, the four glycerol fractions (Gly1 to Gly4) contained RSV virion and NSvc2 protein (Fig 2B). Transmission Electron Microscopy showed that numerous filamentous RSV virion were present in the pellet sample (Fig 2C).

To verify the above findings, SBPHs were fed on a mixture of sucrose and the combined supernatant fraction, combined glycerol fraction, the resuspended pellet sample, or the mixed supernatant and pellet sample through a layer of stretched parafilm membrane for 24 h. As shown in Fig 2D and 2E, NSvc2 (red) and RSV virion (green) were detected together in the epithelial cells of SBPHs fed on the mixture of sucrose and the combined glycerol fraction (Fig 2D, row 2). RSV virion was, however, not detected in the microvillus of SBPHs fed on the mixtures of

sucrose and the combined supernatant fraction or the resuspended pellet sample (Fig 2D, row 1 and 3). In contrast, when insects were allowed to feed on a mixture of sucrose and the combined supernatant fraction plus the resuspended pellet sample, both NSvc2 and RSV virion were detected in the epithelial cells (OC value = 0.95 ± 0.03; Fig 2D, row 4), similar to that found for the SBPHs fed on the mixture of sucrose and the combined glycerol fraction (OC value = 0.97 ± 0.04). Statistical analysis of RSV transmission using SBPHs fed on various samples also indicated that feeding on the mixture of sucrose and the combined supernatant fraction plus the resuspended pellet sample allowed RSV virion entrance into the midgut epithelial cells for a successful virus transmission (Fig 2E). This finding suggests that RSV NSvc2 is a critical factor mediating RSV virion entrance into SBPH midgut cells. To validate the interaction between RSV NP and NSvc2, we performed yeast two-hybrid assays. Results showed that RSV NP interacted with both NSvc2-N and NSvc2-C (Fig 2F). All these data suggested that NSvc2 protein is critical for RSV virion entrance into SBPH midgut.

Recombinant amino-terminal soluble region of NSvc2 directly binds to midgut and inhibits subsequent RSV acquisition by SBPH

Previous studies have shown that NSvc2 can be further processed into two mature glycoproteins, namely amino-terminal and carboxyl-terminal NSvc2 [40]. S1A Fig illustrated the predicted structure of NSvc2 and the positions of its signal peptides, transmembrane regions, and the predicted glycan sites. To examine the potential roles

of amino-terminal NSvc2 (NSvc2-N) in RSV transmission, we expressed the soluble NSvc2-N protein (referenced to as NSvc2-N:S) in Sf9 insect cells using a recombinant baculovirus expression system (S1B Fig). After purification using the Ni-NTA agarose, the expression of the recombinant NSvc2-N:S was confirmed by Western blot assay using an anti-NSvc2-N polyclonal antibody (Fig 3A).

To further determine whether the recombinant NSvc2-N:S protein can bind midgut epidermal microvillus, SBPHs were allowed to feed on purified NSvc2-N:S for 3 h followed by a 12 h feeding on a sucrose solution to remove unbound NSvc2-N:S. Results of immunofluorescence analyses showed that NSvc2-N:S (green signal) could be readily detected in the midgut lumen near the surface of epithelial cells in the alimentary canal (Fig 3B). As a negative control, SBPHs were allowed to feed on *Tomato spotted wilt virus* (TSWV) encoded glycoprotein (Gn:S), known to bind thrip midgets [28]. As expected, the TSWV Gn:S (green) was not detected in SBPH midguts.

Based on the above results, we further hypothesized that the pre-acquired NSvc2-N:S could prevent RSV acquisition by blocking midgut RSV specific receptors. To test this hypothesis, SBPHs were allowed to feed on the purified NSvc2-N:S for 24 h and then on RSV-infected rice plants for 48 h. The alimentary canals were dissected from SBPHs and probed using the RSV NP or NSvc2-N specific antibodies. Under the confocal microscope, the labeled RSV virion was found in the midgut lumen of SBPHs pre-fed with purified NSvc2-N:S (S2A Fig), suggesting that RSV virion was prevented from entering into the midgut epithelial

cells. In contrast, RSV virion was detected in the midgut epithelial cells after the insects were pre-fed with TSWV Gn:S or with sucrose alone (S2B Fig and S2C Fig).

To further confirm the role of NSvc2-N during SBPH acquisition of RSV, SBPHs pre-fed with NSvc2-N:S were allowed to feed on RSV-infected rice plants for 48 h and then on healthy rice seedlings for 12 days. After this feeding period, the insects were tested for RSV infection by ELISA assay. Results showed that pre-feeding SBPHs with NSvc2-N:S did significantly reduce the rate of RSV infection compared with the insects pre-fed with TSWV Gn:S or sucrose only (Fig 3C). This finding indicated that NSvc2-N:S could inhibit RSV entrance into SBPH midgut.

N-glycosylation of NSvc2-N is required for midgut receptor recognition of RSV

Computer-assisted modeling suggested that NSvc2 might be modified through glycosylation (S1A Fig). To confirm this prediction, purified NSvc2-N:S was incubated with PNGaseF (a N-glycosidase) or O-Glycosidases and Neuraminidase (O-Gly + Neur) to remove the N- or O-linked glycans, respectively. Subsequent SDS-PAGE and immunoblotting analyses showed that the purified NSvc2-N:S protein band was shifted in the gel after the PNGaseF treatment, compared with the non-treated NSvc2-N:S (Fig 3D, compare lane1 and 2). No clear band shift was detected when NSvc2-N:S was treated with O-Gly + Neur (Fig 3D, compare lane1 and 3). When NSvc2-N:S was treated with PNGaseF together with O-Gly + Neur, the protein band shifted as that treated with PNGaseF (Fig 3D, compare lane2 and 4),

235 indicating that NSvc2-N was modified by the N-linked glycans.

236 We then generated a NSvc2-N:S site-directed alanine-substitution mutant,
237 NSvc2-N:S$^{N114A/N199A/N232A}$ (N114A/N199A/N232A), at its putative N-linked glycan
238 sites, and a mutant, NSvc2-N:S$^{S38A/S128A/S183A}$ (S38A/S128A/S183A), at its putative
239 O-linked glycan sites. These two mutants were purified as describe above for the
240 wild-type (WT) NSvc2-N:S followed by the enzymatic deglycosylation analyses.
241 Results showed that, without PNGaseF treatment, the NSvc2-N:S$^{N114A/N199A/N232A}$
242 mutant displayed a similar protein band shift in the gel as that shown by the WT
243 NSvc2-N:S treated with PNGaseF (Fig 3E, compare lane 2 and 3). A slight band shift
244 was noticed for the NSvc2-N:S$^{N114A/N199A/N232A}$ mutant, without or with PNGaseF
245 treatment (Fig 3E, compare lane 3 and 4). No O-linked glycan modification was
246 detected for the NSvc2-N:S$^{S38A/S128A/S183A}$ mutant (S38A/S128A/S183A, Fig 3F). This
247 result indicated that residue N114, N199 and N232 of NSvc2-N:S are indeed the
248 N-glycosylation sites.

249 To investigate whether the N-linked glycosylation can affect the recognition of
250 NSvc2-N:S by midgut surface receptors, SBPHs were fed with the two mutant
251 proteins, respectively, for 3 h followed by a 12 h feeding on a sucrose only solution to
252 clean insect alimentary canals. Insects fed with the NSvc2-N:S$^{N114A/N199A/N232A}$ mutant
253 protein showed almost no green labeling signal at the surface of midgut microvillus.
254 In contrast, insects fed with the NSvc2-N:S$^{S38A/S128A/S183A}$ mutant protein did (Fig 3G).
255 ELISA results showed that the NSvc2-N:S$^{N114A/N199A/N232A}$ mutant protein had no
256 obvious effect on SBPH RSV acquisition (Fig 3H). Consequently, we conclude that

modification of NSvc2-N protein through N-glycosylation is important for midgut surface receptor recognition.

RSV virion:NSvc2-N:NSvc2-C complexes enter into the endosomes and NSvc2-C separates from RSV virion:NSvc2-N after releasing from endosomes

Endocytosis is an important process for several circulative-transmitted animal viruses during entering into animal cells [43]. The localization of NSvc2-N and RSV virion suggested that RSV virion and NSvc2-N has entered into endosomal-like vesicle (Fig 1*B* and 1F). To further investigate the localization of RSV virion and NSvc2-N after recognition by SBPH midgut cell receptor(s), early and late endosome specific markers (Rab5, EEA1 and Rab7) were used to visualize these vesicles [44, 45]. Results showed that RSV virion did co-localize with the early endosome Rab5 marker and the late endosome Rab7 marker (Fig 4A and 4B). In the same study, NSvc2-N and carboxyl-terminal protein of NSvc2 (NSvc2-C) were also found to co-localize with early endosome EEA1 marker (Fig 4C and 4D).

To examine the potential role(s) of NSvc2-C, SBPHs were allowed to feed on RSV-infected rice plants for 4, 8, 16 or 24 h, and then used for immunofluorescence labeling assays. NSvc2-C with red labeling signal was observed together with RSV virion (green) at the surface of microvillus (blue) (S3A Fig and S3E Fig; OC value = 0.86 ± 0.04), and in the endosomal-like vesicles in epithelial cells (S3B Fig and S3F Fig; OC value = 0.95 ± 0.03) at 4 and 8 h post feeding. At 16 and 24 h post feeding,

RSV virion (green) had accumulated alone in the cytoplasm of epithelial cells (S3C Fig and S3G Fig [OC value = 0.18 ± 0.02], and S3D Fig and S3H Fig [OC value = 0.32 ± 0.06]), suggesting that NSvc2-C remained inside the endosomal-like vesicles while RSV virion was released from the endosomal-like vesicles and accumulated in the cytoplasm. To confirm this finding, the localization of RSV virion, NSvc2-N and NSvc2-C was examined just at the time that RSV virion release from endosomes. The results showed that after being released from endosomes, NSvc2-N continued to associate with RSV virion in cytosol (Fig 4E, white dashed circles), whereas NSvc2-C stayed inside the actin-labeled endosome and was not released into cytosol of epithelial cells (Fig 4F, white dashed box). This finding indicates that NSvc2-C associates with RSV virion:NSvc2-N in endosome but was separated from them after the virion were released from endosome.

NSvc2-C induces insect cell membrane fusion under acidic conditions

To determine whether NSvc2-N and/or NSvc2-C play roles in membrane fusion, we fused a signal peptide of baculovirus (gp64) to NSvc2-N and NSvc2-C, and expressed these proteins individually in insect *Spodoptera frugiperda* (Sf9) cells by the recombinant baculovirus expression system (Fig 5A). Expressions of these recombinant proteins were confirmed by an immunolabeling assay. Under the laser scanning confocal microscope, red labeling fluorescence signal representing NSvc2-N or NSvc2-C was observed on the Sf9 cell membranes (Fig 5B). We then tested whether NSvc2-N or NSvc2-C could trigger cell membrane fusion under acidic

conditions. Sf9 cells infected with the recombinant NSvc2-N or NSvc2-C baculovirus were treated with a PBS, pH 5.0, for 2 min and then grown in a pH neutral medium. Numerous cell-cell fusions (syncytium) were observed at 4 h post acidic PBS treatment of Sf9 cells infected with the NSvc2-C baculovirus (Fig 5E and 5G). In contrast, no significant cell-cell fusion was observed for cells infected with the NSvc2-N or empty baculovirus (Fig 5C and 5D). In addition, cell membrane fusion was observed in cells co-infected with NSvc2-N and NSvc2-C baculoviruses (Fig 5F and 5G), confirming that RSV NSvc2-C, but not NSvc2-N, played an important role in cell-cell fusion under acidic conditions.

Conserved hydrophobic fusion-loop motifs in NSvc2-C are crucial for fusogenic activity

To further investigate the function of NSvc2-C in cell membrane fusion, we generated a three-dimensional (3D) structure of NSvc2-C through a homology modeling approach (S4A Fig and S4B Fig). This 3D structure consisted of three distinct domains: domain I (yellow), II (red), and III (blue). Two putative fusion loops (green) were found at the top of the 3D structure. Similar fusion loops were reported to be responsible for cell-cell fusion during animal virus infections [46, 47]. In this study, we constructed three NSvc2-C fusion domain deletion mutants (i.e., ΔFL1, ΔFL2 and ΔFL1+ΔFL2), and expressed them individually in Sf9 cells followed by immunoblotting (S4C Fig and S4D Fig). The fusogenic activities of these deletion mutants were then examined in Sf9 cells using the recombinant baculovirus

expression system. Results showed that the number of syncytial cells induced by the ΔFL1 or ΔFL2 mutant was much less than that induced by the WT NSvc2-C (S4E Fig and S4F Fig). The lowest number of syncytial cells was, however, observed in the Sf9 cells infected with the baculovirus carrying the ΔFL1+ΔFL2 double deletion mutant. Based on this finding, we conclude that the two NSvc2-C fusion loops play critical roles in cell-cell fusion.

To identify the amino acid residue(s) important for fusogenic activity, we aligned the RSV fusion loop sequences (Cys459-Cys465, Loop1 and Cys485-Tyr498, Loop 2) with the loop sequences of other four tenuiviruses (Fig 5H). The alignment result indicated that these two fusion loops were relatively conserved among the five tenuiviruses. Six conserved hydrophobic amino acid residues (Phe460, Phe489, Phe492, Tyr494, Pro496 and Tyr498) were found at the unique vertex in the modeled NSvc2-C 3D structure (Fig 5I). Introduction of mutations into these six amino acid residues suggested that three residues (F460A, F489A, and Y498A) were important for membrane fusion activity (Fig 5J and 5K).

NSvc2-C fusogenic-activity-deficient mutant fails to mediate RSV virion release from endosome

The above results showed that RSV NSvc2-N and NSvc2-C had different functions during RSV transmission via SBPH. To elucidate the role of NSvc2-C in RSV entrance into midgut cells during virus acquisition, we analyzed the fusion loop mutants for their functions in RSV virion release from endosome. Purified RSV virion

was incubated for 3 h with Sf9 cell crude extracts containing the full length NSvc2 and then used the mixture to feed SBPHs for 24 h. Midguts were isolated from SBPHs and probed for the presence of RSV virion and NSvc2-N through immunofluorescence labeling. Result showed that RSV virion (green) and NSvc2-N (red) were both present in the endosomal-like vesicles in epithelial cells, indicating that both RSV virion and NSvc2-N had entered into the midgut cells (Fig 6A, upper row). Result also showed that RSV virion was released from endosome at 24 h post feeding. We then prepared Sf9 cell crude extracts containing the N-glycosylation-deficient mutant NSvc2$^{N114A/N199A/N232A}$ or the fusogenic-activity-deficient mutant NSvc2$^{F460A/F489A/Y498A}$. Using the same feeding method described above, RSV virion was detected in the midgut lumen but not in the epithelial cells of SBPHs fed with the mixture of RSV virion and NSvc2$^{N114A/N199A/N232A}$ mutant (Fig 6A, middle row). This study also showed that RSV virion and NSvc2$^{F460A/F489A/Y498A}$ mutant overcame the midgut barrier and entered together into the endosomal-like structures. However, RSV virion and NSvc2$^{F460A/F489A/Y498A}$ mutant were hardly detected in the cytoplasm of epithelial cells. Also, greater number of endosomal-like structures was found in epithelial cells of SBPHs fed with the mixture of RSV virion and NSvc2$^{F460A/F489A/Y498A}$ mutant than that fed with the mixture of RSV virion and wild type NSvc2 (Fig 6A, bottom row). Statistical analysis further confirmed that RSV virion did enter endosomes but failed to be released into cytosol after SBPHs were fed with the mixtures of purified RSV virion and NSvc2$^{F460A/F489A/Y498A}$ mutant, while RSV virion did not enter endosomes

363 when SBPHs were fed with the mixtures of purified RSV virion and
364 NSvc2$^{N114A/N199A/N232A}$ mutant (Fig 6B). This finding indicates that the
365 fusogenic-activity-deficient NSvc2 mutant can mediate virion passage through
366 epithelial cells but failed to release RSV virion from endosomal-like vesicles.

367 # Discussion

368 Understanding how plant viruses are transmitted through their insect vectors in field is
369 one of the key steps to manage virus diseases worldwide. Insect midgut is a major
370 barrier to block the entrance of non-compatible plant viruses. In this study, we used
371 RSV and its SBPH vector as a working model to elucidate the molecular mechanism
372 controlling RSV virion entrance into SBPH midgut for replication. We demonstrated
373 here for the first time that RSV, a circulative and propagative transmitted *Tenuivirus*,
374 used a molecular bridge strategy to overcome the midgut barrier in SBPH for virus
375 persistent transmission.

376 In this study, we confirmed that glycoprotein NSvc2 of RSV is not a structural
377 protein of RSV virion, and found that in the absence of this glycoprotein, RSV virion
378 is unable to overcome the midgut barrier (Fig 2). RSV glycoprotein NSvc2 was
379 further processed into an amino-terminal part protein known as NSvc2-N and a
380 carboxyl-terminal part protein known as NSvc2-C in RSV-infected cells [39, 40]. We
381 found that NSvc2-N accumulated on midgut surface during virus acquisition by SBPH.
382 We also found that the ectopically expressed and purified soluble NSvc2-N:S bound
383 directly to midgut surface and inhibited the subsequent RSV acquisition by SBPH. We

consider that this soluble NSvc2-N:S protein can recognize SBPH midgut surface receptor(s). Our enzymatic deglycosylation result showed that NSvc2-N could be modified by N-linked but not O-linked glycans. The glycan-modification of NSvc2-N might be different from the N- and O-glycosylation of TSWV Gn protein reported previously [28]. It is noteworthy that the N-glycosylation-deficient NSvc2-$N^{N114A/N199A/N232A}$ mutant was unable to interact with midgut surface and to block RSV acquisition by SBPH. Moreover, feeding SBPHs with a mixture of purified RSV virion and crude extract from Sf9 cells expressing full length NSvc2 resulted in a successful transmission of RSV. In contrast, the N-glycosylation-deficient NSvc2 mutant was unable to facilitate RSV virion to pass through SBPH midgut barrier. Therefore, we propose that N-glycosylation modification plays an important role in interaction between RSV virion and SBPH midgut receptor(s). A sugar transporter in SBPH midgut cell was recently found to play critical role in RSV transmission [48]. It would be interested in investigating the interactions between NSvc2 and sugar transporter protein and the biological function of glycosylation for these interactions in the future.

Although the function of RSV glycoprotein NSvc2 was proposed to be similar to that of tospovirus glycoprotein or phytoreovirus spike protein during virus acquisition and transmission [29, 49], NSvc2 is not present on the surface of non-enveloped filamentous RSV virion while both tospovirus glycoprotein and phytoreovirus spike protein are located virion surface. Purified RSV virion is not capable of entering SBPH midgut cells. This inability can, however, be rescued by addition of

406 glycoprotein NSvc2 (Fig 2D and Fig 6A). For non-persistent or semi-persistent
407 transmitted plant viruses, the helper component proteins or helper factors were shown
408 to act as molecular bridges for the interactions between virion and the cuticle of their
409 insect vectors [4, 6]. Although these helper component proteins or factors are not
410 located on the surface of purified virion, these factors are absolutely required for
411 insect transmissions [18, 50]. Our results presented in this paper indicate that this
412 helper factor theory can also be used to explain the function of glycoprotein NSvc2
413 during RSV circulative and propagative transmission by SBPH. First, the RSV
414 glycoprotein NSvc2 is not a virion structural protein (Fig 2). Second, the glycoprotein
415 NSvc2 acts as a molecular bridge to ensure the interaction between RSV virion and
416 SBPH midgut receptor(s) (Fig 3). Third, the glycoprotein NSvc2 is absolutely
417 required for RSV virion entrance into SBPH midgut cells (Fig 2 and Fig 6). These
418 findings strongly supported that RSV glycoprotein NSvc2 is a helper factor protein
419 and this helper factor functions as a molecular bridge to allow the proper interaction
420 between RSV viroin and SBPH midgut during persistent transmission of *Tenuivirus*.

421 After recognition and interaction with RSV virion, midgut epithelial cells
422 underwent endocytosis, resulting in an enclosure of RSV virion:NSvc2 complexes in
423 early and then late endosomes. After that, RSV virion was released from the late
424 endosomes into cytoplasm for replication and for further spreading to other cells.
425 NSvc2-C was initially found together with RSV virion on midgut surface, and later in
426 endosomal-like vesicles. Although NSvc2-C retained inside the endosomes,
427 NSvc2-N-associated RSV virion was released into cytoplasm. We determined that,

under acidic conditions, the expressed NSvc2-C could cause Sf9 cell membrane to fuse. To identify the amino acid residue(s) controlling this membrane fusion activity, a homology based modeling approach was used to create a 3D structure of NSvc2-C followed by site-directed mutagenesis. With the aid of homology modeling, we identified that NSvc2-C residue F460, F489 and Y498 played critical roles during cell membrane fusion. Importantly, the NSvc2 mutant that failed to cause cell membrane fusion was unable to release RSV virion from endosomes into cytoplasm. It is likely that the acidic condition inside endosomes caused conformation change of NSvc2-C, leading to cell membrane fusion. The two fusion loops found in NSvc2 are highly conserved among the members in the genus *Tenuivirus* and are critical for cell membrane fusion induction.

Current gene function studies for plant multi-segmented negative-strand RNA viruses are difficult due mainly to the lack of proper reverse genetics methods. In this paper, we described a new and useful approach to overcome this obstacle. We first expressed the WT or mutant NSvc2 individually in Sf9 insect cells and then incubated the Sf9 cell crude extracts with purified RSV virion. After feeding SBPHs with a WT or mutant NSvc2 extract mixed with purified RSV virion, we successfully determined that virion from the sample containing the WT NSvc2 and purified RSV virion overcame the midgut barrier, entered the epithelial cells, and then released from late endosomes to cytosol for further replication and transmission. The defective NSvc2 mutants failed to interact with midgut surface and thus were unable to mediate the entrance of RSV virion into epithelial cells. In addition, using this approach, we were

able to confirm that the cell membrane fusion defective mutant could not mediate the release of RSV virion from endosomes to cytosol. The assay methods developed in this study should benefit gene function studies for viruses whose infectious clones are currently difficult to make. We proposed that this newly developed technology can not only be used to investigate the functions of tenuivirus glycoproteins, but can also be used to determine the functions of glycoproteins encoded by other plant multi-segmented negative-strand RNA viruses.

Taken together, we conclude that circulative and propagative transmitted RSV uses a molecular bridge strategy to bring RSV virion to SBPH midgut surface during vector transmission. Based on the findings presented in this study, we propose a working model for plant tenuiviruses (Fig 6C). In this model, the NSvc2-N and NSvc2-C do not associate with RSV virion in infected plant cells. After plant sap containing RSV virion, NSvc2-N, and NSvc2-C is acquired into the midgut lumen of SBPH, NSvc2-N recognizes the unidentified midgut cell surface receptor(s) and acts as a molecular bridge to ensure the interaction between RSV virion and midgut surface. Upon attachment of RSV virion:NSvc2-N:NSvc2-C complexes to midgut surface receptor(s), midgut cells undergo endocytosis, resulting in compartmentalization of RSV virion, NSvc2-N, and NSvc2-C in early and then late endosomes. The acidic condition inside the late endosomes triggers a conformation change of NSvc2-C, and the conformation-changed NSvc2-C cause cell membrane to fuse. Finally, the RSV virion:NSvc2-N complexes are released into cytosol (Fig 6C). Findings presented in this paper demonstrate a new type of virus–vector midgut

interaction that requires a virally encoded molecular bridge during virus persistent transmission. This type of mechanism has never been shown for persistent transmitted plant viruses or animal viruses. This new finding expands our understanding of molecular mechanism(s) controlling virus–insect vector interactions during virus transmission in nature.

Materials and methods

Insect and virus maintenance

Rice stripe tenuivirus (RSV) was previously isolated from an RSV-infected rice plant, and maintained inside a growth chamber at the Jiangsu Academy of Agricultural Sciences, Jiangsu Province, China. Small brown planthopper (SBPH) was reared on seedlings of rice cv. Wuyujing NO.3 inside growth incubators set at 26.5 ℃ and a photoperiod of 16 h / 8 h (light / dark). Rice seedlings were changed once every 12 days to ensure sufficient nutrition as described [51].

Isolation of RSV virion

Eight hundred milliliter precooled 0.1 M phosphate buffer (PB), pH7.5, with 0.01 M EDTA was added to 50 g RSV-infected rice leaf tissues followed by 5 min homogenization in a blender. The homogenate was centrifuged at 8,000 × g for 20 min at 4℃. The resulting supernatant was slowly mixed with 6 % PEG 6000 and 0.1 M NaCL, and stirred overnight at 4 ℃. After centrifugation at 8,000 × g for 20 min, the pellet was resuspended in 0.01 M PB and then centrifuged again at 150,000 × g

for 2 h. The pellet was resuspended in 6 ml 0.01 M PB buffer and laid on a 4 ml 20 % glycerol cushion inside a centrifuge tube followed by a centrifugation at 150,000 × *g* for 2 h. Different fractions inside the centrifuge tube were collected individually and the pellet was resuspended in PB buffer (contains 30 % glycerol) prior to storage at -70 ℃.

Immunofluorescence staining of SBPH midgut organs

Immunofluorescence staining assay was performed as described previously with specific modifications [52]. Midguts were obtained from second-instar nymphs and fixed overnight in a 4 % paraformaldehyde (PFA, Thermo Fisher, USA) solution at 4 ℃. After three rinses in a 0.01 M phosphate-buffered saline (PBS), pH 7.4, the midguts were treated for 30 min in a 2 % Triton X-100 solution followed by 1 h incubation in a specific primary antibody. The midguts were then incubated in a specific fluorescence conjugated secondary antibody or a fluorescence conjugated actin antibody for 2 h at room temperature (RT). The midguts were rinsed three times in PBS and mounted in an antifade solution (Solarbio). The mounted midguts were examined under an inverted Leica TCS SP8 fluorescent confocal microscope (Leica Microsystems, Solms, Germany). LAS X software was used to analyze fluorescence spectra to determine co-localization of two proteins.

Rabbit polyclonal antibody against RSV NSvc2-N or NSvc2-C was produced in our laboratory. Mouse monoclonal antibody against RSV NP was a gift from Professor Jianxiang Wu, Zhejiang University, Hangzhou, China. Primary antibodies also used in

this study included Rab5 anti-rabbit IgG (C8B1; Cell Signaling Technology), Rab7 anti-rabbit IgG (D95F2; Cell Signaling Technology), and EEA1 anti-mouse IgG (NBP2-36568; Novus). Secondary antibodies used in this study were FITC conjugated rabbit anti-mouse IgG (F9137; Sigma) or goat anti-rabbit IgG (F9887; Sigma), TRITC conjugated goat anti-rabbit IgG (T6778; Sigma), Alexa Fluor 647 phalloidin (A22287; Invitrogen) or Rhodamine Phalloidin (R415; Invitrogen).

Recombinant baculovirus expression in insect cell

Construction of recombinant baculovirus was the same as described previously [53]. Sequence encoding RSV NSvc2-N:S (amino acid positions 20 to 265, lacking the signal peptide and the transmembrane domain) was PCR-amplified using a cDNA from a RSV-infected rice plant. The resulting PCR fragment represented the RSV NSvc2-N:S sequence and a six-His tag sequence at its 3' end terminus. The Gp64 signal peptide sequence was then fused to the 5' end terminus of NSvc2-N:S sequence via overlapping PCR. The final PCR product was cloned into vector pFastBac1 (S1 Table). The site-directed mutagenized mutants were constructed as described [54]. All plasmids were sequenced, transformed individually into DH10Bac^{TM} cells to generate recombinant baculoviruses as instructed by the manufacturer (Invitrogen). The recombinant baculoviruses were co-transfected individually with the FnGENE HD Transfection Reagent (Promega) into *Spodoptera frugiperda* (Sf9) cells to obtain the stable expression of recombinant baculoviruses.

Expression and purification of soluble proteins

534 Sf9 cells were infected with recombinant baculoviruses at a multiplicity of infection
535 (MOI) of five, and the infected-cells were collected at 72 h post infection. The
536 infected-cells were lysed in 10 ml PBS using a ultrasonic cell crusher followed by
537 centrifugation at 4 ℃ to remove cell debris. After centrifugation, the supernatant was
538 collected, incubated with nickel-nitrilotriacetic acid resin (Ni-NTA, Germany) for 2 h,
539 and then loaded onto a chromatographic column (Bio-Rad Hercules, California). After
540 separation, the column was washed with two bed volumes of 50 mM imidazole in
541 PBS, and the recombinant protein was eluted with 250 mM imidazole followed by
542 dialysis against PBS prior to storage at -70 ℃ until use.

543 **Glycosylation and Immunoblotting assays**

544 Purified NSvc2-N:S and various mutant proteins were deglycosylated with PNGaseF
545 as instructed (NEB, USA) to remove N-linked glycans or Neuraminidase and
546 O-Glycosidase (NEB, USA) to remove O-linked glycans. Proteins were mixed with
547 0.5 % SDS and 40 mM DTT, and incubated at 100℃ for 10 min. After denaturation,
548 buffer and glycosidases were added to the samples and incubated for 3 h at 37 ℃. The
549 enzyme-treated samples were mixed with a loading buffer containing SDS and boiled
550 for 10 min prior to electrophoresis in 10 % (w/v) SDS-PAGE gels. The separated
551 proteins were transferred to nitrocellulose membranes and the membranes were
552 probed with a polyclonal rabbit antibody against NSvc2-N (1:5,000 dilution) and then
553 a goat anti-rabbit IgG HRP conjugate (31466; Invitrogen). The detection signal was
554 visualized using the ChemiDoc^{TM} Touch Imaging System (Bio-Rad, Hercules,

555 California).

556 Glycoprotein midgut binding assays

557 Midgut binding assays were performed as described previously [28]. Briefly,
558 second-instar nymphs were placed in open-ended EP centrifuge tubes and fed with
559 mixtures of purified glycoproteins resuspended in a TF buffer (PBS with 10 %
560 glycerol, 0.01 % Chicago sky blue, and 5 mg / ml BSA) through a stretched parafilm
561 membrane. After 3 h feeding, the glycoprotein mixtures were replaced with a 10 %
562 sucrose solution for another 12 h feeding to clear midguts, indicated by the
563 disappearance of the Chicago sky blue dye from the midguts. The insects were then
564 dissected, fixed in PFA and analyzed by immunofluorescence staining as described
565 above.

566 Detection of SBPH RSV acquisition using Enzyme linked
567 immunosorbent assay (ELISA)

568 Second-instar nymphs were placed in an empty bottle for 2 h and then allowed to
569 acquire purified protein through a stretched parafilm membrane for 24 h. The pre-fed
570 SBPHs were then allowed to feed on RSV-infected rice seedlings for 48 h prior to
571 feeding on healthy rice seedlings for another 12 days. SBPHs were transferred
572 individually into a centrifuge tube and grinded thoroughly in PBS buffer. After brief
573 centrifugation, individual supernatant samples were blotted on nitrocellulose
574 membranes and the membranes were probed with a 1:5,000 (v/v) diluted monoclonal

antibody against RSV NP, and then a 1:20,000 diluted secondary alkaline phosphatase (AP)-coupled goat anti-mouse IgG (Sigma). Detection signal was visualized using a 5-bromo-4-chloro-3-indo-lylphosphate-nitroblue tetrazolium (BCIP-NBT) solution (Sangon Biotech, Shanghai, China). Three independent experiments with 50 nymphs / treatment were performed.

Yeast two-hybrid assay

Yeast two-hybrid assays were performed according to the instructions from the manufacturer (Clontech, TaKaRa, Japan). Briefly, one bait vector and a specific prey vector, described in the result section, were co-transformed into the Y2HGold strain cells by heat shock method. In addition, vector pGADT7-T was co-transformed into the Y2HGold strain cells with vector pGBKT7-53 or vector pGBKT7-Lam, and used as a positive and a negative control, respectively. All co-transformed cells were first grown on a synthetic dextrose medium lacking Tryptophan and Leucine amino acid (SD-Trp-Leu) for 3 days at 30 ℃, and then on a synthetic dextrose medium lacking Tryptophan, Leucine, Histidine and Ademethionine amino acid (SD-Trp-Leu-His-Ade) for 5 days at 30 ℃.

Low pH-induced membrane fusion assay

Sf9 cells were infected with different recombinant baculoviruses at a MOI of five for 48 h. The infected cells were washed twice with fresh medium, treated with a PBS buffer, pH 5.0, for 2 min and then in a pH neutral medium. The cells were incubated

595 for 4 h at 28 ℃ and then examined for the cell-cell membrane fusion under an
596 Olympus IX71 inverted fluorescence microscope (Olympus, Hamburg, Germany).

597 Homology modeling of NSvc2-C

598 Homology based modeling of NSvc2-C was as described previously [55, 56]. Briefly,
599 RSV NSvc2-C sequence was used to search the I-TASSER Server software. Based on
600 the high TM-score value (0.805), glycoprotein of *Sever Fever with Thrombocytopenia*
601 *Syndrome Phlebovirus* (SFTSV) (PDB: 5G47) was chosen as the template to build the
602 homology based model of RSV NSvc2-C. Amino acid residues and their surface
603 displays in the three-dimensional structure were predicted using the PyMOL program.

604 Acknowledgments

605 We thank Prof. Yidong Wu (College of Plant Protection, Nanjing Agricultural
606 University, China) for kindly providing the insect Sf9 cell lines. We also thank Prof.
607 Tong Zhou (Institute of Plant Protection, Jiangsu Academy of Agricultural Sciences)
608 for kindly providing the RSV-infected rice samples.

609

610 References

611 1. Gray SM, Banerjee N. Mechanisms of arthropod transmission of plant and animal viruses.
612 Microbiol Mol Biol R. 1999; 63:128-48. PMID: 10066833.
613 2. Ruckert C, Weger-Lucarelli J, Garcia-Luna SM, Young MC, Byas AD, Murrieta RA, et al. Impact
614 of simultaneous exposure to arboviruses on infection and transmission by Aedes aegypti mosquitoes.
615 Nat commun. 2017; 8: 15412. doi: 10.1038/ncomms15412 PMID: 28524874.

3. Dader B, Then C, Berthelot E, Ducousso M, Ng JCK, Drucker M. Insect transmission of plant viruses: Multilayered interactions optimize viral propagation. Insect Sci. 2017; 24: 929-46. doi: 10.1111/1744-7917.12470 PMID: 28426155.
4. Ng JC, Falk BW. Virus-vector interactions mediating nonpersistent and semipersistent transmission of plant viruses. Annu Rev Phytopathol. 2006; 44: 183-212. doi: 10.1146/annurev.phyto.44.070505.143325 PMID: 16602948.
5. Hogenhout SA, Ammar ED, Whitfield AE, Redinbaugh MG. Insect vector interactions with persistently transmitted viruses. Annu Rev Phytopathol. 2008; 46: 327-59. doi: 10.1146/annurev.phyto.022508.092135 PMID: 18680428.
6. Whitfield AE, Falk BW, Rotenberg D. Insect vector-mediated transmission of plant viruses. Virology. 2015; 479: 278-89. doi: 10.1016/j.virol.2015.03.026 PMID: 25824478.
7. Childress SA, Harris KF. Localization of Virus-Like Particles in the Foreguts of Viruliferous Graminella-Nigrifrons Leafhoppers Carrying the Semi-Persistent Maize Chlorotic Dwarf Virus. J Gen Virol. 1989; 70: 247-51. doi: 10.1099/0022-1317-70-1-247.
8. Martin B, Collar JL, Tjallingii WF, Fereres A. Intracellular ingestion and salivation by aphids may cause the acquisition and inoculation of non-persistently transmitted plant viruses. J Gen Virol. 1997; 78: 2701-5. doi: 10.1099/0022-1317-78-10-2701 PMID: 9349493.
9. Chen AY, Walker GP, Carter D, Ng JC. A virus capsid component mediates virion retention and transmission by its insect vector. Proc Natl Acad Sci USA. 2011; 108: 16777-82. doi: 10.1073/pnas.1109384108 PMID: 21930903.
10. Blanc S, Drucker M, Uzest M. Localizing viruses in their insect vectors. Annu Rev Phytopathol. 2014; 52: 403-25. doi: 10.1146/annurev-phyto-102313-045920 PMID: 24996011.
11. Gray S, Cilia M, Ghanim M. Circulative, "nonpropagative" virus transmission: an orchestra of virus-, insect-, and plant-derived instruments. Adv Virus Res. 2014; 89: 141-99. doi: 10.1016/B978-0-12-800172-1.00004-5 PMID: 24751196.
12. Pirone TP, Blanc S. Helper-dependent vector transmission of plant viruses. Annu Rev Phytopathol. 1996; 34: 227-47. doi: 10.1146/annurev.phyto.34.1.227 PMID: 15012542.
13. Ng JCK, Zhou JS. Insect vector-plant virus interactions associated with non-circulative, semi-persistent transmission: current perspectives and future challenges. Curr Opin Virol. 2015; 15: 48-55. doi: 10.1016/j.coviro.2015.07.006 PMID: 26318639.
14. Uzest M, Gargani D, Drucker M, Hebrard E, Garzo E, Candresse T, et al. A protein key to plant virus transmission at the tip of the insect vector stylet. Proc Natl Acad Sci USA. 2007; 104: 17959-64. doi: 10.1073/pnas.0706608104 PMID: 17962414.
15. Webster CG, Pichon E, van Munster M, Monsion B, Deshoux M, Gargani D, et al. Identification of Plant Virus Receptor Candidates in the Stylets of Their Aphid Vectors. J Virol. 2018; 92: e00432-18. doi: 10.1128/JVI.00432-18 PMID: 29769332.
16. Atreya CD, Pirone TP. Mutational Analysis of the Helper Component-Proteinase Gene of a Potyvirus - Effects of Amino-Acid Substitutions, Deletions, and Gene Replacement on Virulence and Aphid Transmissibility. Proc Natl Acad Sci USA. 1993; 90: 11919-23. doi: 10.1073/pnas.90.24.11919 PMID: 8265648.
17. Blanc S, Ammar ED, Garcia-Lampasona S, Dolja VV, Llave C, Baker J, et al. Mutations in the potyvirus helper component protein: effects on interactions with virions and aphid stylets. J Gen Virol. 1998; 79: 3119-22. doi: 10.1099/0022-1317-79-12-3119 PMID: 9880030.
18. Ruiz-Ferrer V, Boskovic J, Alfonso C, Rivas G, Llorca O, Lopez-Abella D, et al. Structural analysis

of tobacco etch potyvirus HC-Pro oligomers involved in aphid transmission. J Virol. 2005; 79: 3758-65. doi: 10.1128/Jvi.79.6.3758-3765.2005 PMID: 15731269.

19. Lung MC, Pirone TP. Acquisition factor required for aphid transmission of purified cauliflower mosaic virus. Virology. 1974; 60: 260-4. PMID: 4841178.
20. Leh V, Jacquot E, Geldreich A, Hermann T, Leclerc D, Cerutti M, et al. Aphid transmission of cauliflower mosaic virus requires the viral PIII protein. EMBO J. 1999; 18: 7077-85. doi: 10.1093/emboj/18.24.7077 PMID: 10601029.
21. Drucker M, Froissart R, Hebrard E, Uzest M, Ravallec M, Esperandieu P, et al. Intracellular distribution of viral gene products regulates a complex mechanism of cauliflower mosaic virus acquisition by its aphid vector. Proc Natl Acad Sci USA. 2002; 99: 2422-7. doi: 10.1073/pnas.042587799 PMID: 11842201.
22. Brault V, Vandenheuvel JFJM, Verbeek M, Zieglergraff V, Reutenauer A, Herrbach E, et al. Aphid Transmission of Beet Western Yellows Luteovirus Requires the Minor Capsid Read-through Protein P74. EMBO J. 1995; 14: 650-9. PMID: 7882968.
23. Gray S, Gildow FE. Luteovirus-aphid interactions. Annu Rev Phytopathol. 2003; 41: 539-66. doi: 10.1146/annurev.phyto.41.012203.105815 PMID: 12730400.
24. Azzam O, Frazer J, Delarosa D, Beaver JS, Ahlquist P, Maxwell DP. Whitefly transmission and efficient ssDNA accumulation of bean golden mosaic geminivirus require functional coat protein. Virology. 1994; 204: 289-96. doi: 10.1006/viro.1994.1533 PMID: 8091659.
25. Noris E, Vaira AM, Caciagli P, Masenga V, Gronenborn B, Accotto GP. Amino acids in the capsid protein of tomato yellow leaf curl virus that are crucial for systemic infection, particle formation, and insect transmission. J Virol. 1998; 72: 10050-7. PMID: 9811744.
26. Tomaru M, Maruyama W, Kikuchi A, Yan J, Zhu Y, Suzuki N, et al. The loss of outer capsid protein P2 results in nontransmissibility by the insect vector of rice dwarf phytoreovirus. J Virol. 1997; 71: 8019-23. PMID: 9311898.
27. Wei TY, Li Y. Rice Reoviruses in Insect Vectors. Annu Rev Phytopathol. 2016; 54: 99-120. doi: 10.1146/annurev-phyto-080615-095900 PMID: 27296147.
28. Whitfield AE, Ullman DE, German TL. Expression and characterization of a soluble form of Tomato spotted wilt virus glycoprotein G(N). J Virol. 2004; 78: 13197-206. doi: 10.1128/Jvi.78.23.13197-13206.2004 PMID: 15542672.
29. Sin SH, McNulty BC, Kennedy GG, Moyer JW. Viral genetic determinants for thrips transmission of Tomato spotted wilt virus. Proc Natl Acad Sci USA. 2005; 102: 5168-73. doi: 10.1073/pnas.0407354102 PMID: 15753307.
30. Redinbaugh MG, Hogenhout SA. Plant rhabdoviruses. Curr Top Microbiol Immunol. 2005; 292: 143-63. PMID: 15981471.
31. Ammar ED, Tsai CW, Whitfield AE, Redinbaugh MG, Hogenhout SA. Cellular and Molecular Aspects of Rhabdovirus Interactions with Insect and Plant Hosts. Annu Rev Entomol. 2009; 54: 447-68. doi: 10.1146/annurev.ento.54.110807.090454 PMID: 18793103.
32. Hibino H. Biology and epidemiology of rice viruses. Annu Rev Phytopathol. 1996; 34: 249-74. doi: 10.1146/annurev.phyto.34.1.249 PMID: 15012543.
33. Cho WK, Lian S, Kim SM, Park SH, Kim KH. Current Insights into Research on Rice stripe virus. Plant Pathol J. 2013; 29: 223-33. doi: 10.5423/PPJ.RW.10.2012.0158 PMID: 25288949.
34. Cifuentes-Munoz N, Salazar-Quiroz N, Tischler ND. Hantavirus Gn and Gc Envelope Glycoproteins: Key Structural Units for Virus Cell Entry and Virus Assembly. Viruses. 2014; 6:

1801-22. doi: 10.3390/v6041801 PMID: 24755564.

35. Spiegel M, Plegge T, Pohlmann S. The Role of Phlebovirus Glycoproteins in Viral Entry, Assembly and Release. Viruses. 2016; 8: 202-21. doi: 10.3390/v8070202 PMID: 27455305.
36. Ramirez BC, Haenni AL. Molecular biology of tenuiviruses, a remarkable group of plant viruses. J Gen Virol. 1994; 75: 467-75. doi: 10.1099/0022-1317-75-3-467 PMID: 8126445.
37. Falk BW, Tsai JH. Biology and molecular biology of viruses in the genus Tenuivirus. Annu Rev Phytopathol. 1998; 36: 139-63. doi: 10.1146/annurev.phyto.36.1.139 PMID: 15012496.
38. Huo Y, Chen LY, Su L, Wu Y, Chen XY, Fang RX, et al. Artificial feeding Rice stripe virus enables efficient virus infection of Laodelphax striatellus. J Virol Methods. 2016; 235: 139-43. doi: 10.1016/j.jviromet.2016.06.003 PMID: 27283882.
39. Zhao S, Zhang G, Dai X, Hou Y, Li M, Liang J, et al. Processing and intracellular localization of rice stripe virus Pc2 protein in insect cells. Virology. 2012; 429: 148-54. doi: 10.1016/j.virol.2012.04.018 PMID: 22575054.
40. Yao M, Liu XF, Li S, Xu Y, Zhou YJ, Zhou XP, et al. Rice stripe tenuivirus NSvc2 glycoproteins targeted to the golgi body by the N-terminal transmembrane domain and adjacent cytosolic 24 amino acids via the COP I- and COP II-dependent secretion pathway. J Virol. 2014; 88: 3223-34. doi: 10.1128/Jvi.03006-13 PMID: 24390331.
41. Toriyama S. Characterization of Rice Stripe Virus: a heavy component carrying infectivity. J Gen Virol. 1982; 61: 187-95. doi: 10.1099/0022-1317-61-2-187.
42. Toriyama S. An RNA-dependent RNA-polymerase associated with the filamentous nucleoproteins of rice stripe virus. J Gen Virol. 1986; 67: 1247-55. doi: 10.1099/0022-1317-67-7-1247.
43. Mercer J, Schelhaas M, Helenius A. Virus entry by endocytosis. Annu Rev Biochem. 2010; 79: 803-33. doi: 10.1146/annurev-biochem-060208-104626 PMID: 20196649.
44. Saeed MF, Kolokoltsov AA, Albrecht T, Davey RA. Cellular entry of ebola virus involves uptake by a macropinocytosis-like mechanism and subsequent trafficking through early and late endosomes. PLoS Pathog. 2010; 6: e1001110. doi: 10.1371/journal.ppat.1001110 PMID: 20862315.
45. Xia WQ, Liang Y, Chi Y, Pan LL, Zhao J, Liu SS, et al. Intracellular trafficking of begomoviruses in the midgut cells of their insect vector. PLoS Pathog. 2018; 14: e1006866. doi: 10.1371/journal.ppat.1006866 PMID: 29370296.
46. Podbilewicz B. Virus and cell fusion mechanisms. Annu Rev Cell Dev Biol. 2014; 30: 111-39. doi: 10.1146/annurev-cellbio-101512-122422 PMID: 25000995.
47. Halldorsson S, Behrens AJ, Harlos K, Huiskonen JT, Elliott RM, Crispin M, et al. Structure of a phleboviral envelope glycoprotein reveals a consolidated model of membrane fusion. Proc Natl Acad Sci USA. 2016; 113: 7154-9. doi: 10.1073/pnas.1603827113 PMID: 27325770.
48. Qin FL, Liu WW, Wu N, Zhang L, Zhang ZK, Zhou XP, et al. Invasion of midgut epithelial cells by a persistently transmitted virus is mediated by sugar transporter 6 in its insect vector. PLoS Pathog. 2018; 14: e1007201. doi: 10.1371/journal.ppat.1007201 PMID: 30052679.
49. Zhou F, Pu Y, Wei T, Liu H, Deng W, Wei C, et al. The P2 capsid protein of the nonenveloped rice dwarf phytoreovirus induces membrane fusion in insect host cells. Proc Natl Acad Sci USA. 2007; 104: 19547-52. doi: 10.1073/pnas.0708946104 PMID: 18042708.
50. Hoh F, Uzest M, Drucker M, Plisson-Chastang C, Bron P, Blanc S, et al. Structural insights into the molecular mechanisms of cauliflower mosaic virus transmission by its insect vector. J Virol. 2010; 84: 4706-13. doi: 10.1128/jvi.02662-09 PMID: 20181714.
51. Li S, Wang S, Wang X, Li X, Zi J, Ge S, et al. Rice stripe virus affects the viability of its vector

offspring by changing developmental gene expression in embryos. Sci Rep. 2015; 5:7883. doi: 10.1038/srep07883 PMID: 25601039.

52. Chen Q, Chen HY, Mao QZ, Liu QF, Shimizu T, Uehara-Ichiki T, et al. Tubular structure induced by a plant virus facilitates viral spread in its vector insect. PLoS Pathog. 2012; 8: e1003032. doi: 10.1371/journal.ppat.1003032 PMID: 23166500.

53. Kost TA, Condreay JP, Jarvis DL. Baculovirus as versatile vectors for protein expression in insect and mammalian cells. Nat Biotechnol. 2005; 23: 567-75. doi: 10.1038/nbt1095 PMID: 15877075.

54. Zhu M, Jiang L, Bai BH, Zhao WY, Chen XJ, Li J, et al. The intracellular immune receptor sw-5b confers broad-spectrum resistance to tospoviruses through recognition of a conserved 21-amino acid viral effector epitope. Plant Cell. 2017; 29: 2214-32. doi: 10.1105/tpc.17.00180 PMID: 28814646.

55. Li J, Feng Z, Wu J, Huang Y, Lu G, Zhu M, et al. Structure and function analysis of nucleocapsid protein of tomato spotted wilt virus interacting with RNA using homology modeling. J Biol Chem. 2015; 290: 3950-61. doi: 10.1074/jbc.M114.604678 PMID: 25540203.

56. Lu G, Li J, Zhou YJ, Zhou XP, Tao XR. Model-based structural and functional characterization of the Rice stripe tenuivirus nucleocapsid protein interacting with viral genomic RNA. Virology. 2017; 506: 73-83. doi: 10.1016/j.virol.2017.03.010 PMID: 28359901.

766 **Figure Legends**

767 **Fig 1. NSvc2 associates with RSV virion in SBPH midgut.** (A) NSvc2 (Red) and
768 RSV virion (green) were co-localized in midgut lumen and on the surface of intestinal
769 microvillus (blue) at 4 h post feeding on RSV-infected rice plants. The presence of
770 RSV virion, NSvc2, and actin were detected with antibodies specific for RSV NP,
771 NSvc2-N, or actin. The boxed regions are shown on the right side of the
772 corresponding images with three panels. The detection signal for NSvc2 is in red, the
773 detection single for virion is in green and the merged detection signal is in yellow. (B)
774 Co-localization of NSvc2 and RSV virion in vesicle-like structures in epithelial cells
775 at 8 h post feeding. (C) Co-localization of NSvc2 and RSV virion in cytoplasm of
776 epithelial cells at 16 h post feeding. (D) NSvc2 and RSV virion complexes were
777 detected in epithelial cells of midgut at 24 h post feeding. (E–H) Analyses of
778 overlapped fluorescence spectra from NSvc2 (red) and RSV virion (green) at different
779 stages. Fluorescence signals were from the white dashed line indicated areas. The
780 overlap coefficient (OC) values were determined individually using the LAS X
781 software. ML, midgut lumen; EC, epithelial cell; Bar, 25 μm.

782

783 **Fig 2. NSvc2 protein is required for RSV entrance into SBPH midgut.** (A) NSvc2
784 is absent in purified RSV virion. Extract from RSV-infected rice plants was loaded on
785 the top of 4 mL 20 % glycerol. The supernatant fractions, glycerol fractions and the
786 pellet were collected after ultra-centrifugation. (B) The fractions were analyzed in gels
787 followed by Coomassie blue staining or by immunoblotting using antibodies specific
788 for RSV NP or NSvc2-N. Sizes of the protein bands are shown on the left. Asterisk

789 indicates a RSV NP dimer. (C) Morphology of RSV virion in a resuspended pellet
790 sample examined by Electron Microscopy. Arrows indicate filamentous RSV virion.
791 Bar, 50 nm. (D) Immunofluorescence labeling of NSvc2 (red) and RSV virion (green)
792 in SBPH midguts after feeding with the combined supernatant fraction, glycerol
793 fraction, resuspended pellet or the supernatant fraction and resuspended pellet mixture.
794 The boxed regions are enlarged and shown on the right side of the merged images.
795 Overlapping fluorescence spectra analyses were done for the white dashed line
796 indicated areas shown in the right panels. The overlap coefficient (OC) values were
797 determined using the LAS X software. ML, midgut lumen; EC, epithelial cell; Bar, 25
798 μm. (E) Statistic analysis of RSV infection in SBPH after feeding on different
799 fractions. Each bar represents three independent biological repeats from each
800 experiment (n=50 / group). **, $p < 0.01$ by student *t*-test analysis. (F) Yeast
801 two-hybrid assay for the interactions between RSV NP and NSvc2-N, or between
802 RSV NP and NSvc2-C. RSV NP was fused to a GAL4 activation domain (AD-NP),
803 and NSvc2-N or NSvc2-C was fused to a GAL4 binding domain (BD-NSvc2-N,
804 BD-NSvc2-C). Yeast cells were co-transformed with indicated plasmids, and were
805 assayed for protein interactions on synthetic dextrose -Trp/-Leu/-His/-Ade medium.
806
807 **Fig 3. N-glycosylation of NSvc2-N is essential for the recognition of midgut**
808 **surface receptor.** (A) Immunoblot analysis of NSvc2-N:S expression in Sf9 cells.
809 Sizes of protein markers are indicated on the left and the NSvc2-N:S protein band is
810 indicated with an arrow. (B) Binding of purified NSvc2-N:S to microvillus surface of

811 SBPH midgut. Arrows indicate the accumulation of NSvc2-N:S (green, left panel) in
812 midgut lumen. Purified TSWV Gn:S was used as a negative control in this study
813 (right panel). ML, midgut lumen; EC, epithelial cell; Bar, 25 μm. (C) Percentages of
814 RSV acquisition by SBPHs pre-fed with NSvc2-N:S, TSWV Gn:S, or sucrose only.
815 All experiments were performed three times (50 SBPHs for each group). ** $p < 0.01$
816 by *t*-test analysis. (D–F) Enzymatic de-glycosylation of NSvc2-N:S. Purified
817 NSvc2-N:S was incubated with PNGaseF or O-Glycosidase + Neuraminidase (O-Gly
818 + Neur) to determine the types of glycans (D). PNGaseF was used to remove the
819 N-linked glycans, and O-Gly + Neur were used to remove the O-linked glycans.
820 N-glycosylation (E) and O-glycosylation (F) of the triple asparagine mutant
821 (NSvc2-N:S$^{N114A/N199A/N232A}$) or triple serine mutant (NSvc2-N:S$^{S38A/S128A/S183A}$) were
822 conducted as described for NSvc2-N:S. The NSvc2-N:S$^{N114A/N199A/N232A}$ mutant was
823 treated with PNGaseF while the NSvc2-N:S$^{S38A/S128A/S183A}$ mutant was treated with
824 O-Gly + Neur. (G) The NSvc2-N:S$^{N114A/N199A/N232A}$ mutant failed to bind SBPH
825 midgut (left) but the O-glycosylated NSvc2-N:S$^{S38A/S128A/S183A}$ mutant did (right). ML,
826 midgut lumen; EC, epithelial cell; Bar, 25 μm. (H) RSV acquisition by SBPHs after
827 pre-feeding with different protein samples. The experiment was repeated three times
828 with 50 SBPHs each group. **, $p < 0.01$ by *t*-test analysis.
829
830 **Fig 4. RSV virion, NSvc2-N and NSvc2-C are co-localized with early or late**
831 **endosomes, and NSvc2-C separates from RSV virion and NSvc2-N complexes**
832 **after releasing from endosomes in midgut epithelial cells.** (A and B) RSV virion

was detected in early endosomes labeled with the Rab5 antibody (A) or in late endosomes labeled with the Rab7 antibody (B) in midgut epithelial cells. Co-localizations of RSV virion with Rab5 or Rab7 or actin in different endosomes are indicated by arrows. ML, midgut lumen; EC, epithelial cell; Bar, 25 μm. (C and D) NSvc2-N and NSvc2-C were detected in early endosomes labeled with the EEA1 antibody in epithelial cells. Co-localizations of NSvc2-N or NSvc2-C with EEA1 or actin in different endosomes are indicated by arrows. Bar, 25 μm. (E) RSV virion and NSvc2-N were released from endosome into the cytosol of epithelial cells. The white dashed cycles indicated a region that RSV and NSvc2-N were detected in the cytosol while actin-labeled endosome was absent. Bar, 25 μm. (F) RSV virion but not NSvc2-C was released from the late endosome in epithelial cells. The white dashed boxes indicated a region that RSV virion was just released from the endosome while NSvc2-C proteins were still associated with actin-labeled endosome. Bar, 25μm.

Fig 5. NSvc2-C hydrophobic fusion-loop motifs are required for cell-cell membrane fusion. (A) Schematic diagrams showing recombinant NSvc2-N and NSvc2-C. Baculovirus gp64 signal peptide was used to replace the original signal peptide at the N-terminus of NSvc2-N or NSvc2-C. (B) Immunofluorescence labeling of the recombinant NSvc2-N or NSvc2-C in Sf9 cells. Sf9 cells were infected with baculoviruses carrying the recombinant NSvc2-N or NSvc2-C (MOI=5). The infected cells were probed with the NSvc2-N or NSvc2-C specific antibody at 48 h post infection followed by a TRITC fluorescent-labeled secondary antibody. Bar, 10 μm.

855 (C–F) Fusogenic activity assays using Sf9 cells expressing the recombinant NSvc2-N,
856 NSvc2-C or both (NSvc2-N + NSvc2-C). The Sf9 cells were infected with
857 recombinant baculoviruses (MOI=5). After 48 h post infection, and the growth
858 medium was replaced with a PBS, pH 5.0, for 2 min and then changed back to the
859 normal growth medium for 4 h. Formation of syncytium was observed under a
860 microscope. (G) The number of cells showing syncytium was counted under the
861 microscope. The experiment was repeated three times. **, $p < 0.01$ by the student
862 *t*-test analysis. (H) Sequence alignment using the two fusion loop sequences (FL1 and
863 FL2) from NSvc2-C of five different tenuiviruses (RSV, MSV, RHBV, IWSV and
864 RGSV). Red residues are highly conserved and yellow residues are semi-conserved.
865 Residues indicated with asterisks are hydrophobic residues and were selected for the
866 site-directed mutagenesis. The resulting mutants were later tested for their abilities to
867 induce cell-cell membrane fusion. (I) Two fusion loops (FL1 and FL2, green) were
868 found at the top of the 3D-structure model of NSvc2-C. Three different domains are
869 shown in three different colors, and the boxed region on the 3D-structure is enlarged
870 and shown on the right side. Locations of the hydrophobic residues are displayed. (J
871 and K) Analyses of the fusogenic activities caused by the WT or mutant NSvc2-C. Sf9
872 cells were infected with recombinant baculoviruses carrying the WT or mutant
873 NSvc2-C for membrane fusion assay (J). The number of cells showing syncytium was
874 recorded and analyzed (K). The experiments were repeated three times. **, $p < 0.01$.
875
876 **Fig 6. NSvc2 functions as a molecular bridge to mediate RSV virion entrance into**

877 **SBPH midgut cell.** (A) Crude extract of Sf9 cell expressing WT NSvc2,
878 NSvc2$^{N114A/N199A/N232A}$ or NSvc2$^{F460A/F489A/Y498A}$ was incubated with purified RSV
879 virion for 3 h at 4 ℃, and then used to feed SBPHs for 24 h. Insect midguts were
880 dissected and detected for RSV virion and NSvc2-N using specific antibodies. The
881 boxed regions in the left column were enlarged and shown in the second to fifth
882 columns on the right. The white circled areas show the release of RSV virion (green)
883 and NSvc2-N (red) from endosome into cytosol. The actin labeling signal is shown in
884 blue. ML, midgut lumen; EC, epithelial cell; Bar, 25 μm. (B) Statistical analysis of
885 RSV infection in SBPH epithelial cells after feeding on the mixtures containing
886 purified RSV virion and the WT or mutant NSvc2-C. Each bar represents three
887 independent biological repeats from each experiment with 50 SBPHs per treatment.
888 **, $p < 0.01$ by student *t*-test analysis.
889

890 **Fig 7. Working model for RSV virion entrance into SBPH midgut cells.** During
891 SBPH feeding on RSV-infected rice plants, RSV virion, NSvc2-N and NSvc2-C are
892 acquired by the vector and enter insect midgut lumen (Step I). After reaching
893 microvillus surface of midgut lumen, NSvc2-N protein directs the
894 virion:NSvc2-N:NSvc2-C complexes to microvillus surface through recognizing the
895 unidentified microvillus surface receptor(s) (Steps II and III). The complexes-attached
896 midgut lumen membrane undergoes endocytosis and compartmentalizes RSV virion,
897 NSvc2-N and NSvc2-C in vesicles (Steps IV and V). These vesicles further develop
898 into early endosomes (Step VI) and then late endosomes (Step VII). The acidic

899 condition inside the late endosomes triggers NSvc2-C to induce cell-cell membrane
900 fusion (Step VII). Finally, RSV virion:NSvc2-N complexes are released from the late
901 endosomes into the cytosol of epithelial cells for further RSV spread in midgut cells
902 (Step VIII).

Supporting information

S1 Fig. Schematic diagram showing the full length NSvc2 (A) and the recombinant soluble NSvc2-N (NSvc2-N:S) (B). Locations of the putative signal peptide, hydrophobic domains, and glycosylation sites are indicated. The signal peptide of NSvc2-N:S is replaced with the signal peptide of Gp64.

S2 Fig. The effects of pre-incubation with purified NSvc2-N:S (A), TSWV Gn:S (B) and sucrose alone (C) on RSV entrance into SBPH midguts. The boxed regions are enlarged and shown on the right side. The overlapping fluorescence spectra were from the white dashed line indicated areas (right top and bottom panels). EC, epithelial cell; Bar, 25 μm.

S3 Fig. Time course study of NSvc2-C subcellular localization during RSV entrance into SBPH midgut. (A) NSvc2-C was co-localized with RSV virion on midgut microvillus surface (blue) at 4 h post feeding on RSV-infected seedlings. The boxed region was enlarged and shown on the right side. The labeled NSvc2-C is shown in red and the labeled RSV virion is shown in green. (B) NSvc2-C and RSV virion were co-localized in the endosomal-like vesicles in midgut epithelial cells at 8 h post infestation. (C) RSV virion was detected in cytoplasm of epithelial cells at 16 h post infestation but not NSvc2-C. (D) NSvc2-C was again not detected together with RSV virion at 24 h post infestation. (E–H) Analyses of overlapping fluorescence spectra from the white dashed lines indicated regions in the merged images. The

925 overlap coefficient (OC) values were determined by the LAS X software. ML, midgut
926 lumen; EC, epithelial cell; Bar, 10 μm.
927
928 **S4 Fig. NSvc2-C hydrophobic fusion-loop motifs are required for cell-cell**
929 **membrane fusion.** (A) A diagram showing different NSvc2-C domains. Different
930 domains are shown in yellow (domain I), red (domain II) and blue color (domain III).
931 Fusion loops (FL1 and FL2) are shown in green, and a hydrophobic region in gray. (B)
932 A three dimensional homology based model of NSvc2-C with the same color
933 arrangement as shown in (A). (C) Schematic representations of the wild type and FL
934 deletion NSvc2-C mutants. Locations of FL1 (black) and FL2 (gray) are shown.
935 Deletions of one or double FLs are indicated with upward open arrows. (D)
936 Expressions of FLAG-tagged WT or mutant NSvc2-C in Sf9 cells were determined by
937 immunoblotting. The blots were probed with a FLAG-specific antibody. Arrows
938 indicate the bands of the expressed NSvc2-C proteins. (E and F) Analyses of
939 fusogenic activities of the WT or mutant NSvc2-C. Sf9 cells were infected with
940 recombinant baculoviruses carrying the WT or deletion mutants. At 48 h post
941 infection, the cells were treated with PBS, pH5.0, for the cell-cell membrane fusion
942 assays (E). The numbers of cells showing syncytium were recorded and analyzed (F).
943 The experiment was repeated three times. **, $p < 0.01$.
944
945 **S1 Table. Primers used in this study**
946

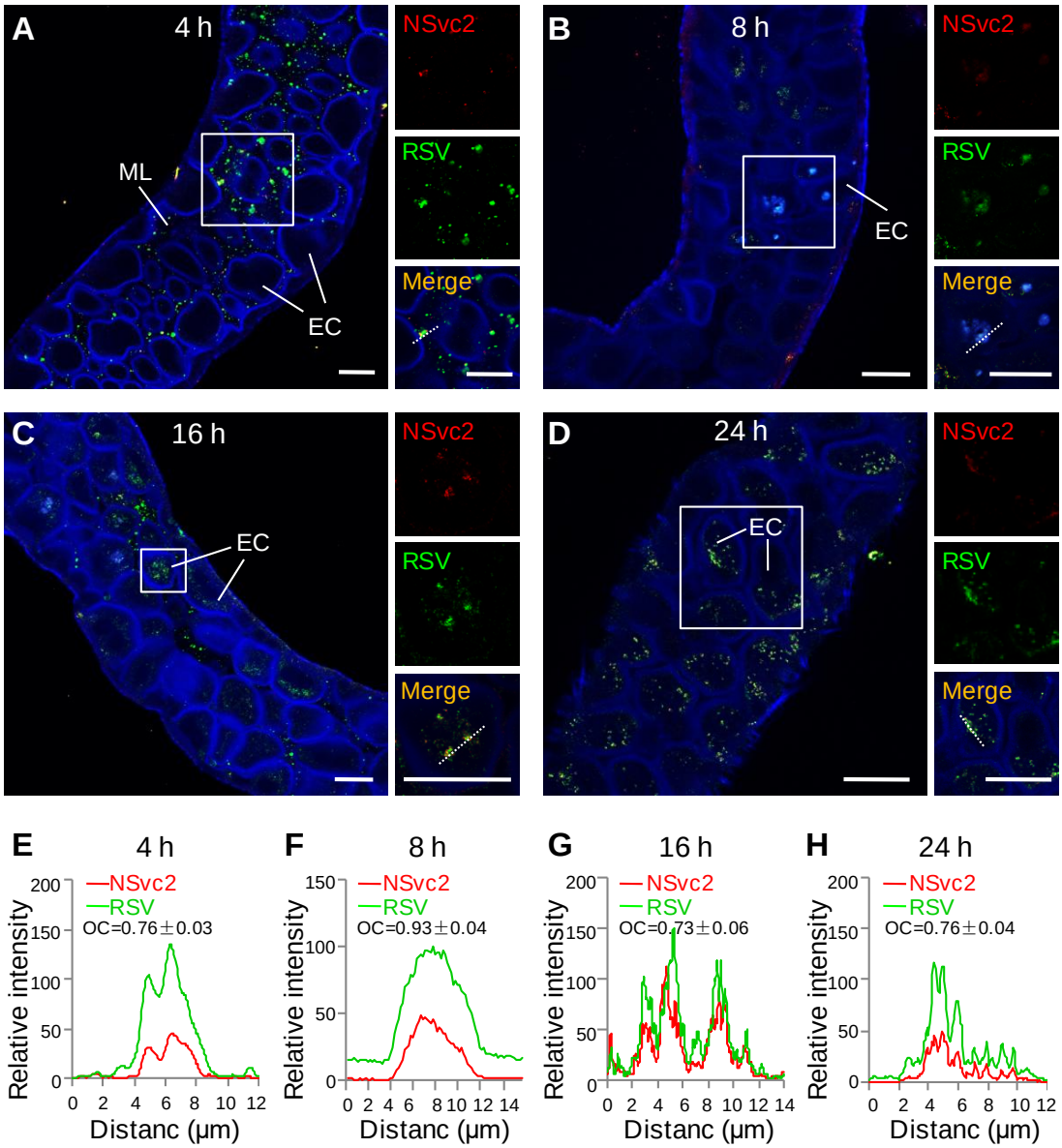

Fig 1.

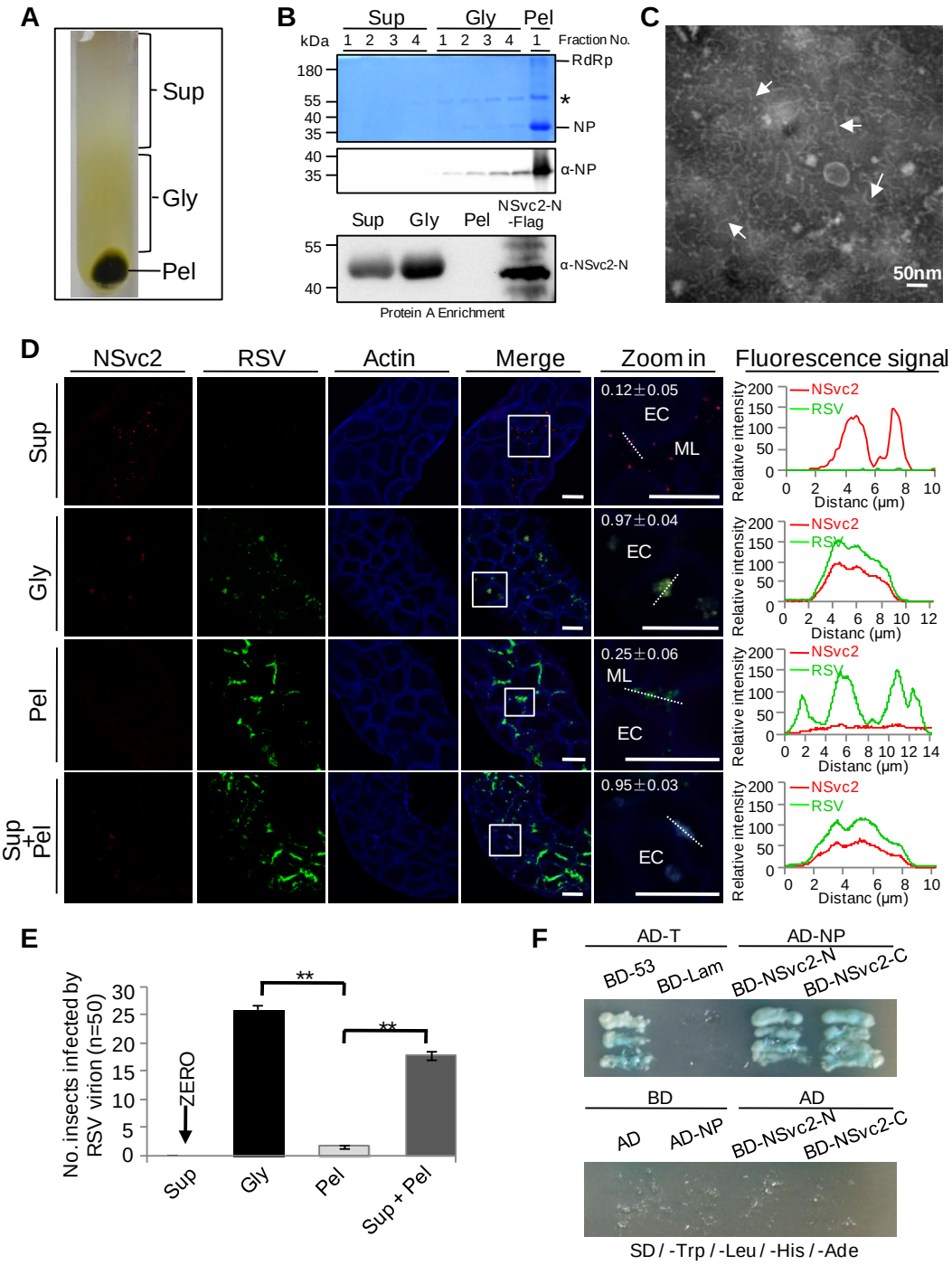

950

951 **Fig 2.**

952

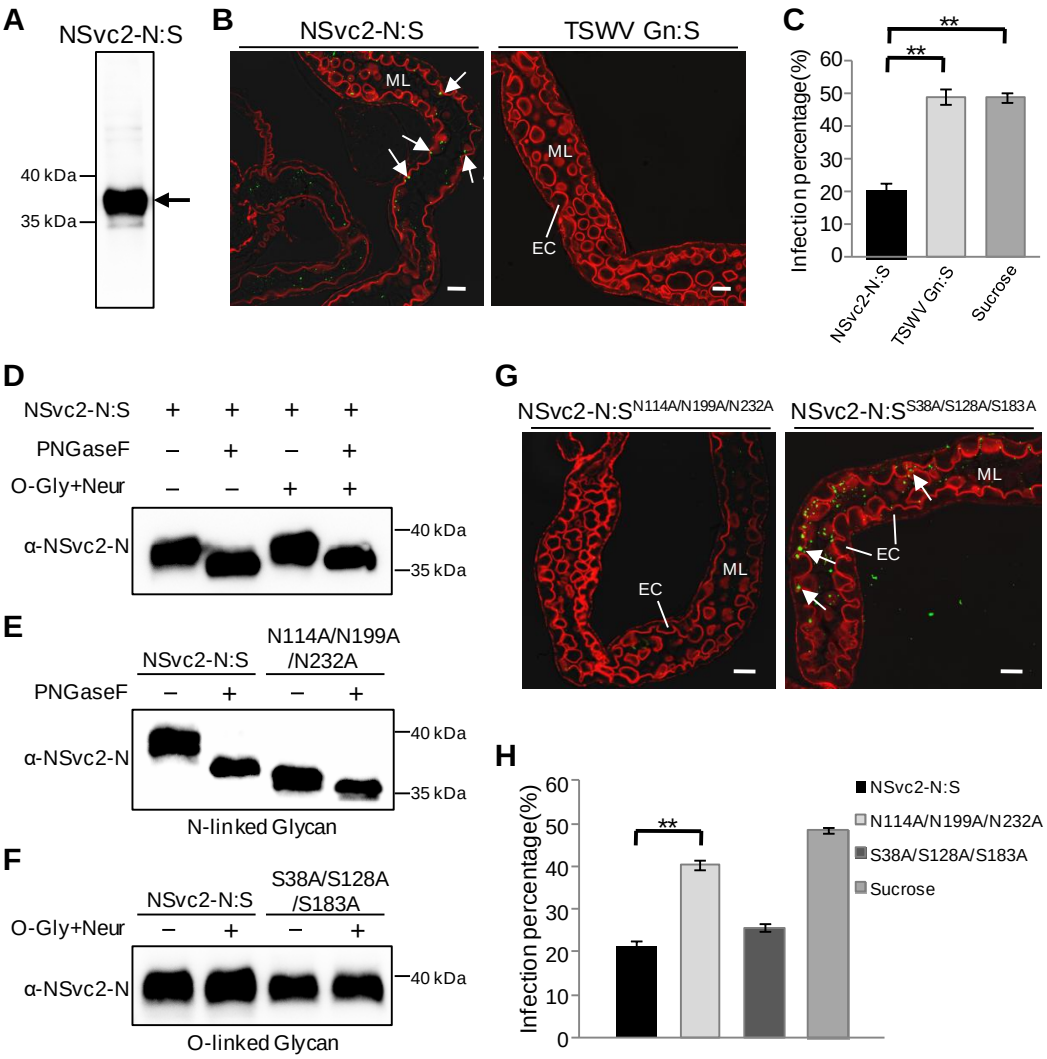

Fig 3.

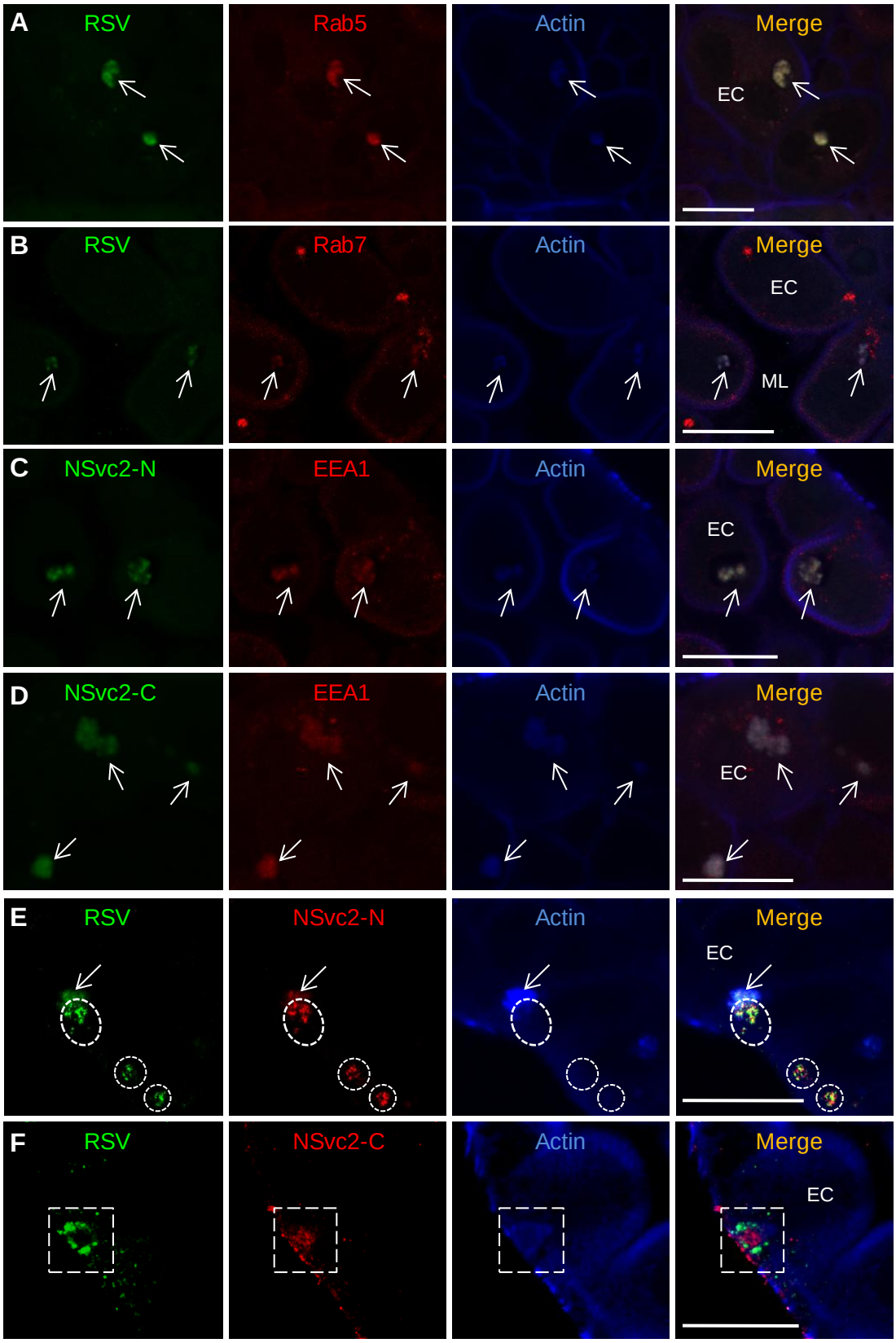

Fig 4.

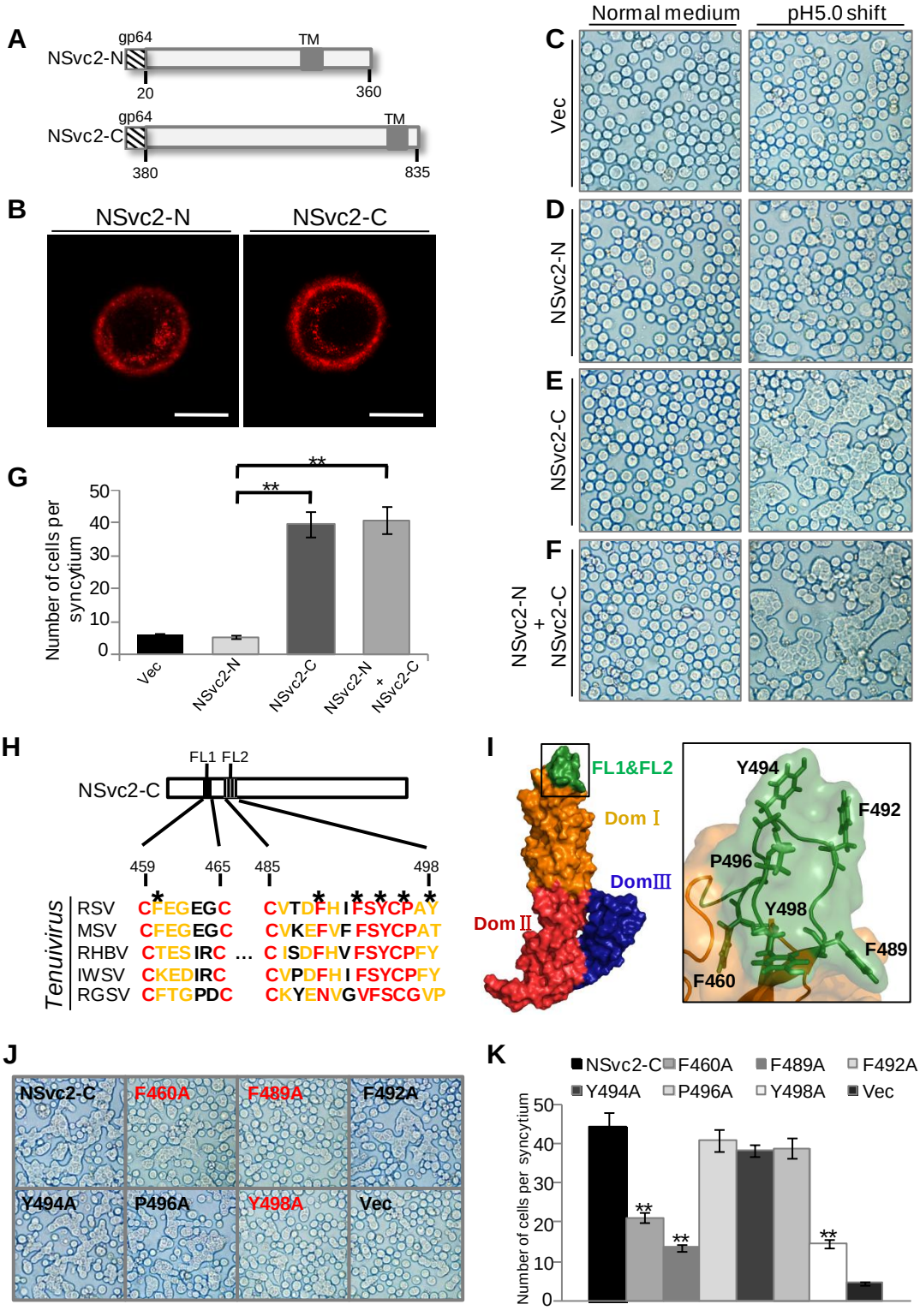

Fig 5.

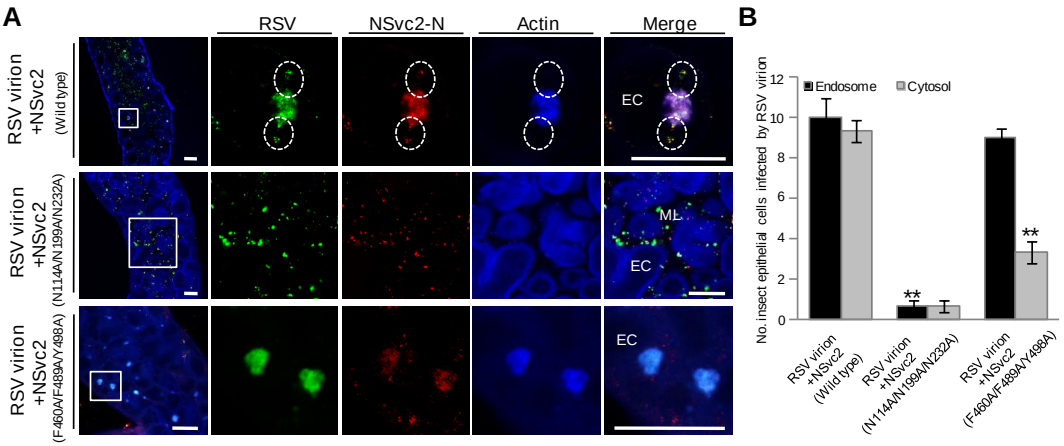

962

963 **Fig 6.**

964

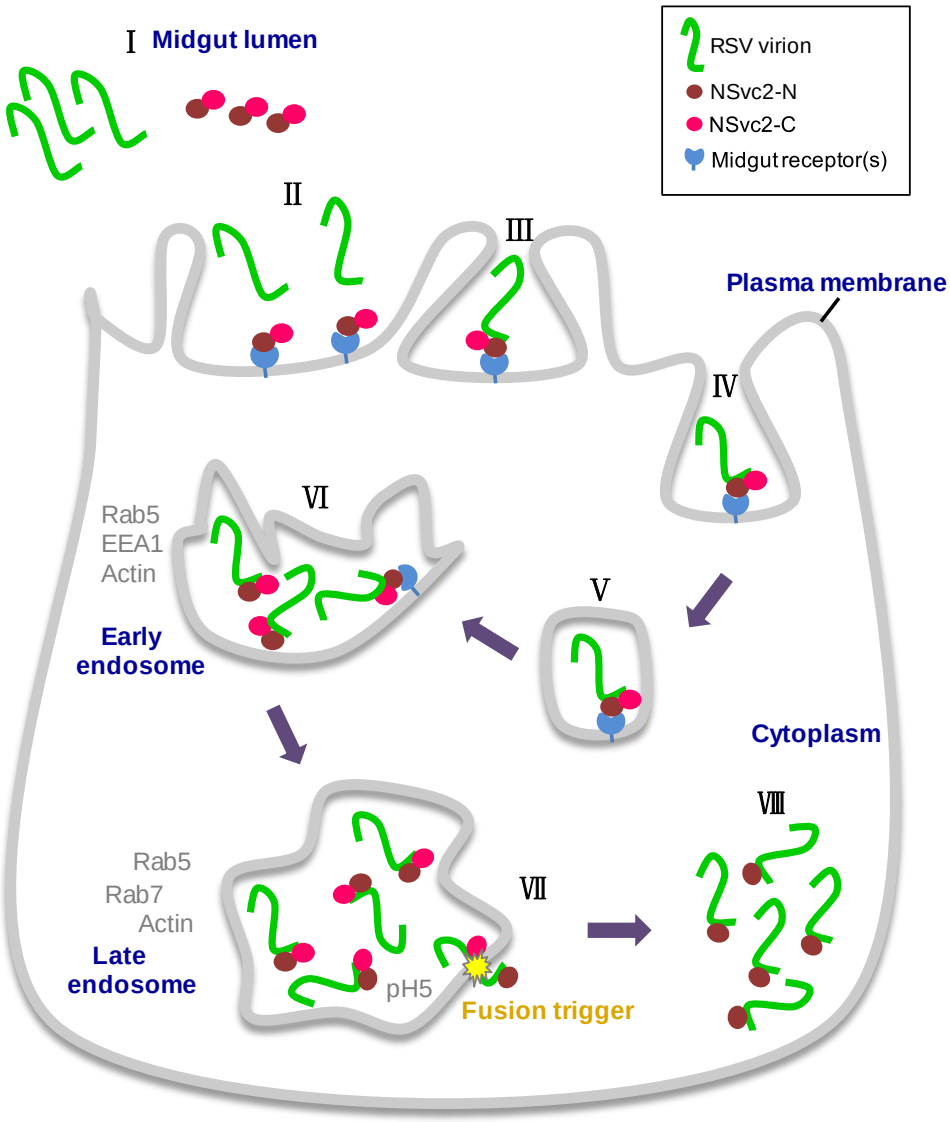

965

966 **Fig 7.**

967

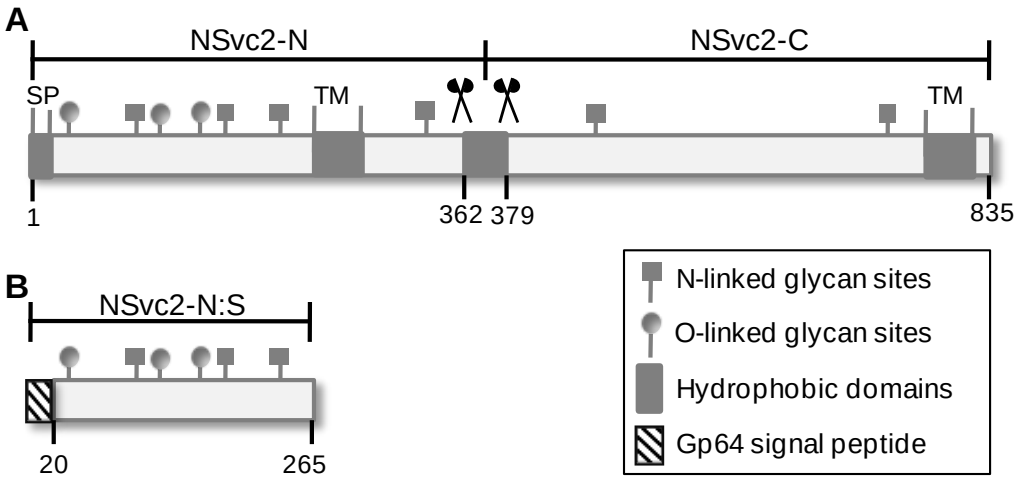

968

969 **S1 Fig.**

970

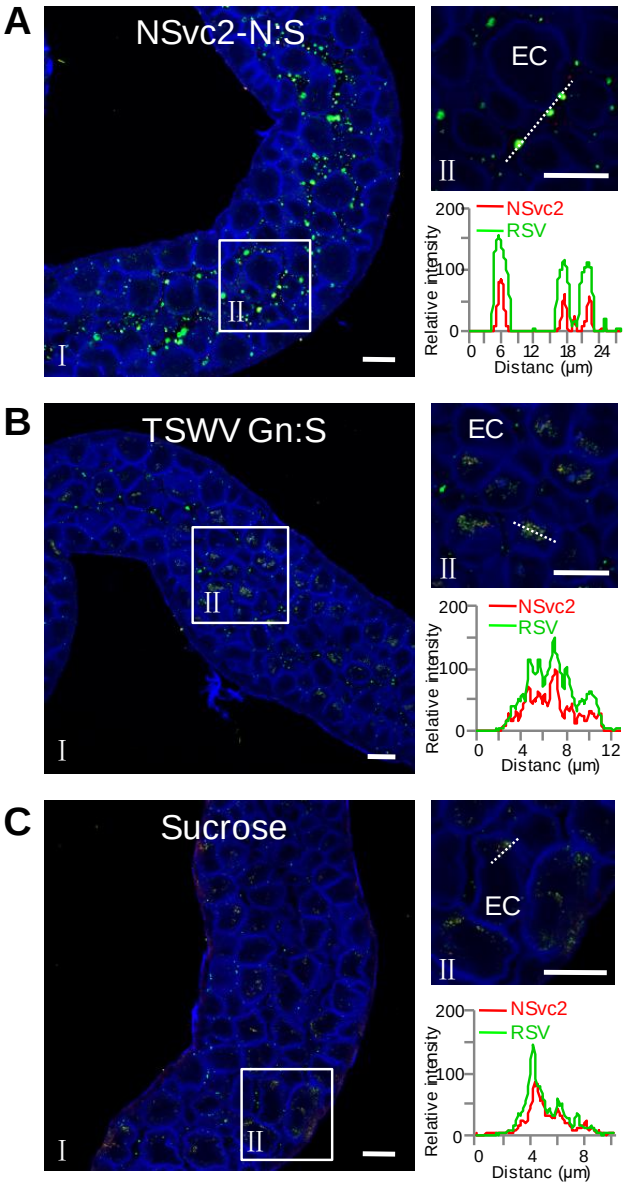

971

972 **S2 Fig.**

973

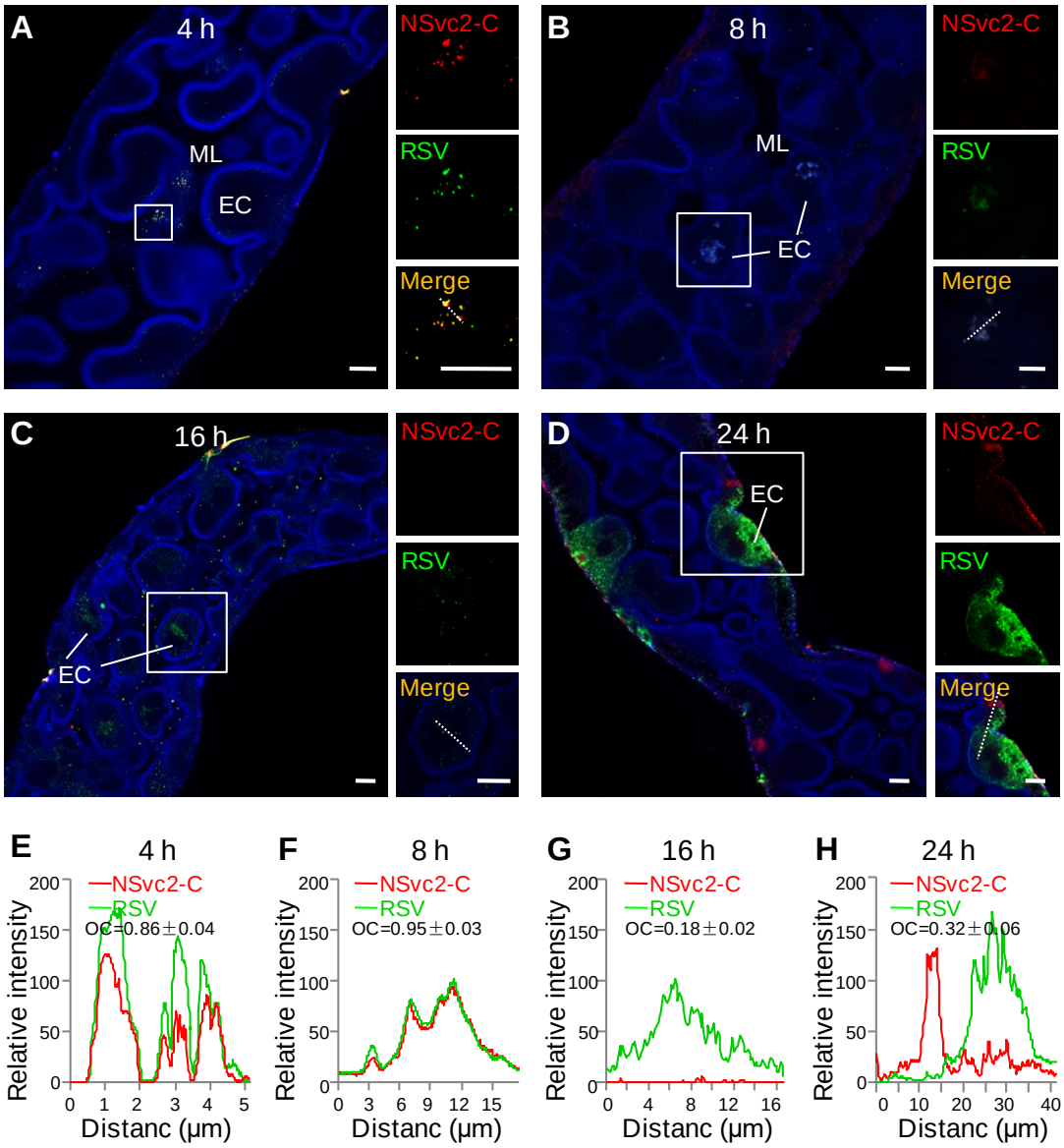

974

975 **S3 Fig.**

976

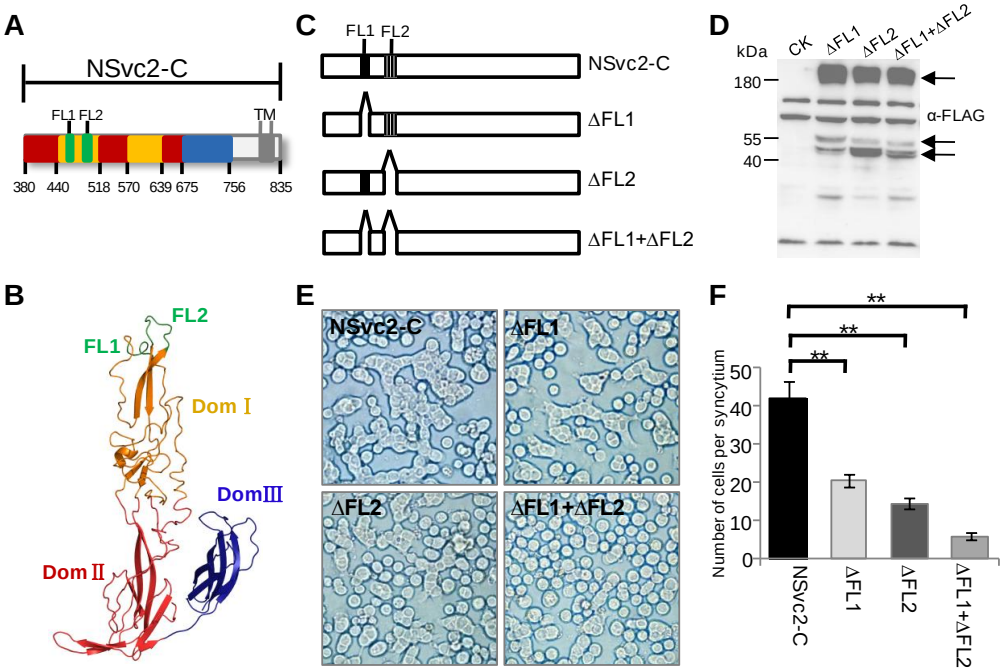

977

978 **S4 Fig.**

979

980 **S1 Table.**

Clone	Primer		Primer sequence (from 5' to 3')	Purpose
pFastbac1-GP64-6xhis-NSvc2-N:S-6xhis	F	P3209	CCggatccATGCACCACCACCACCACCACCCAATACCTTTCCCTGACAC	To amplify RSV NSvc2-N:S fragment (20-265aa) and GP64 fragment, then clone into pFastbac1
	R	P3210	CCGctcgagTCAGTGGTGGTGGTGGTGGTGTGAATATCTATAGATGTGAG	
	F	P3253	CGggatccATGGTAAGCGCTATTGTTTT	
	R	P3254	GAagatctGTTGCAGTGCTCCGCCGCAA	
pFastbac1-GP64-6xhis-TSWV-Gn:S-6xhis	F	P3391	CCggatccATGCACCACCACCACCACCACGCTAAAGTAGAAATAATTCG	To amplify TSWV Gn:S fragment (35-300aa) and GP64 fragment, then clone into pFastbac1
	R	P3392	CCGctcgagTCAGTGGTGGTGGTGGTGGTGTCTGACTCTTTTGTTTGTTT	
	F	P3253	CGggatccATGGTAAGCGCTATTGTTTT	
	R	P3254	GAagatctGTTGCAGTGCTCCGCCGCAA	
pFastbac1-GP64-NSvc2-N-1xFlag	F	LG-1	CGGAGCACTGCAACAGATCCatggcaccaataccttccc	To amplify two fragments and do homologous recombination to obtain plasmid
	R	LG-2	gggaaaggtattggtgccatGGATCTGTTGCAGTGCTCCG	
	F	LG-3	agggtaggaaagtagagaatGATTACAAGGATGATGATGA	
	R	LG-4	TCATCATCATCCTTGTAATCattctctactttcctaccct	
pFastbac1-GP64-NSvc2-C-1xFlag	F	P4500	CGggatccATGGAATCCTGTCAAGACCTTG	To amplify RSV NSvc2-C and GP64 fragments, then clone into pFastbac1
	R	P4501	CGctcgagTTA*CTTATCATCATCATCCTTGTAATC*ATCAACCTGTCTAATGTC	
	F	P3253	CGggatccATGGTAAGCGCTATTGTTTT	
	R	P3254	GAagatctGTTGCAGTGCTCCGCCGCAA	
pFastbac1-GP64-NSvc2-C(ΔFL1)-1xFlag	F	P4726	CCACCATCGGGCGCGGATCCatggtaagcgctattgtttt	To amplify deletion mutant fragment and vector fragment, then do homologous recombination to obtain plasmid
	R	P4727	aaaacaatagcgcttaccatGGATCCGCGCCCGATGGTGG	
	F	P4563	agagaggaatggaaaAGAACTGATGGAACA	
	R	P4564	tgttccatcagttctTTTCCATTCCTCTCT	
pFastbac1-GP64-NSvc2-C(ΔFL2)-1xFlag	F	P3253	CGggatccATGGTAAGCGCTATTGTTTT	To amplify NSvc2-C deletion mutant fragments, then mix the two fragments and do overlap PCR to obtain the mutant and clone into pFastbac1
	R	P4565	ctgagctttgattatCACTACAATTGGAAG	
	F	P4566	cttccaattgtagtgATAATCAAAGCTCAG	
	R	P4501	CGctcgagTTA*CTTATCATCATCATCCTTGTAATC*ATCAACCTGTCTAATGTC	

pFastbac1-GP64-NSvc2-C(ΔFL1 & ΔFL2)-1xFlag	F	P4726	CCACCATCGGGCGCGGATCCatggtaagcgctattgtttt	To amplify deletion mutant fragment and vector fragment, then do homologous recombination to obtain plasmid
	R	P4727	aaaacaatagcgcttaccatGGATCCGCGCCCGATGGTGG	
	F	P4565	ctgagctttgattatCACTACAATTGGAAG	
	R	P4566	cttccaattgtagtgATAATCAAAGCTCAG	
pFastbac1-GP64-NSvc2-C(F460A)-1xFlag	F	P4726	CCACCATCGGGCGCGGATCCatggtaagcgctattgtttt	To amplify point mutant fragment and vector fragment, then do homologous recombination to obtain plasmid
	R	P4727	aaaacaatagcgcttaccatGGATCCGCGCCCGATGGTGG	
	F	P2603	GAGGAATGGAAATGT*gct*GAAGGGGAAGGTTGC	
	R	P2604	GCAACCTTCCCCTTC*agc*ACATTTCCATTCCTC	
pFastbac1-GP64-NSvc2-C(F489A)-1xFlag	F	P4726	CCACCATCGGGCGCGGATCCatggtaagcgctattgtttt	To amplify point mutant fragment and vector fragment, then do homologous recombination to obtain plasmid
	R	P4727	aaaacaatagcgcttaccatGGATCCGCGCCCGATGGTGG	
	F	P2605	TATTGTGTCACTGAT*gcc*CACATATTTTCCTAT	
	R	P2606	ATAGGAAAATATGTG*ggc*ATCAGTGACACAATA	
pFastbac1-GP64-NSvc2-C(F492A)-1xFlag	F	P4726	CCACCATCGGGCGCGGATCCatggtaagcgctattgtttt	To amplify point mutant fragment and vector fragment, then do homologous recombination to obtain plasmid
	R	P4727	aaaacaatagcgcttaccatGGATCCGCGCCCGATGGTGG	
	F	P2607	GTCACTGATTTCCACGCA*gct*TCCTATTGCCCAGCA	
	R	P2608	TGCTGGGCAATAGGA*agc*TGCGTGGAAATCAGTGAC	
pFastbac1-GP64-NSvc2-C(F494A)-1xFlag	F	P4726	CCACCATCGGGCGCGGATCCatggtaagcgctattgtttt	To amplify point mutant fragment and vector fragment, then do homologous recombination to obtain plasmid
	R	P4727	aaaacaatagcgcttaccatGGATCCGCGCCCGATGGTGG	
	F	P2609	TTCCACATATTTTCC*gct*TGCCCAGCATACCAC	
	R	P2610	GTGGTATGCTGGGCA*agc*GGAAAATATGTGGAA	
pFastbac1-GP64-NSvc2-C(F496A)-1xFlag	F	P4726	CCACCATCGGGCGCGGATCCatggtaagcgctattgtttt	To amplify point mutant fragment and vector fragment, then do homologous recombination to obtain plasmid
	R	P4727	aaaacaatagcgcttaccatGGATCCGCGCCCGATGGTGG	
	F	P2611	ATATTTTCCTATTGC*gca*GCATACCACTACAAT	
	R	P2612	ATTGTAGTGGTATGC*tgc*GCAATAGGAAAATAT	

pFastbac1-GP64-NSvc2-C(F498A)-1xFlag	F	P4726	CCACCATCGGGCGCGGATCCatggtaagcgctattgtttt	To amplify point mutant fragment and vector fragment, then do homologous recombination to obtain plasmid
	R	P4727	aaaacaatagcgcttaccatGGATCCGCGCCCGATGGTGG	
	F	P2613	TCCTATTGCCCAGCA*gcc*CACTACAATTGGAAG	
	R	P2614	CTTCCAATTGTAGTG*ggc*TGCTGGGCAATAGGA	
pFastbac1-GP64-6xHis-NSvc2-N(N114A/N199A/N232)-6xHis	F	P4726	CCACCATCGGGCGCGGATCCatggtaagcgctattgtttt	To amplify point mutant fragment and vector fragment, then do homologous recombination to obtain plasmid
	R	P4727	aaaacaatagcgcttaccatGGATCCGCGCCCGATGGTGG	
	F	LG-5	GATGCTATTCTGCAG*gct*GTATCTCTGGTTGGC	
	R	LG-6	GCCAACCAGAGATAC*agc*CTGCAGAATAGCATC	
	F	LG-7	TCTGCATGTGAGGTC*gct*GTGAGTGACCAGACA	
	R	LG-8	TGTCTGGTCACTCAC*agc*GACCTCACATGCAGA	
	F	LG-9	AAGGGTGGTTGTCAA*gct*GTTACTTGTCACCCA	
	R	LG-10	TGGGTGACAAGTAAC*agc*TTGACAACCACCCTT	
pFastbac1-GP64-6xHis-NSvc2-N(S38A/S128A/S183A)-6xHis	F	P4726	CCACCATCGGGCGCGGATCCatggtaagcgctattgtttt	To amplify point mutant fragment and vector fragment, then do homologous recombination to obtain plasmid
	R	P4727	aaaacaatagcgcttaccatGGATCCGCGCCCGATGGTGG	
	F	LG-11	AGGGAGAGAGTTCCA*gct*GAGATTGTCAAGGTC	
	R	LG-12	GACCTTGACAATCTC*agc*TGGAACTCTCTCCCT	
	F	LG-13	ACAGAATACACATCA*gct*CCTCTATTGATAACT	
	R	LG-14	AGTTATCAATAGAGG*agc*TGATGTGTATTCTGT	
	F	LG-15	GTTGCAATCAAGCCC*gct*TGCACAGATGGTGTG	
	R	LG-16	CACACCATCTGTGCA*agc*GGGCTTGATTGCAAC	
pFastbac1-GP64-6xHis-NSvc2-1xFlag	F	P3209	CCggatccATGCACCACCACCACCACCACCCAATACCTTTCCCTGACAC	To amplify RSV NSvc2 and GP64 fragments, then clone into pFastbac1
	R	P4501	CGctcgagTTA*CTTATCATCATCATCCTTGTAATC*ATCAACCTGTCTAATGTC	
	F	P3253	CGggatccATGGTAAGCGCTATTGTTTT	
	R	P3254	GAagatctGTTGCAGTGCTCCGCCGCAA	
pFastbac1-GP64-6xHis-NSvc2(N114A/N199A/N232A)-1xFlag	F	P4726	CCACCATCGGGCGCGGATCCatggtaagcgctattgtttt	To amplify point mutant fragment and vector fragment, then do homologous recombination to obtain plasmid
	R	P4727	aaaacaatagcgcttaccatGGATCCGCGCCCGATGGTGG	
	F	LG-5	GATGCTATTCTGCAG*gct*GTATCTCTGGTTGGC	
	R	LG-6	GCCAACCAGAGATAC*agc*CTGCAGAATAGCATC	
	F	LG-7	TCTGCATGTGAGGTC*gct*GTGAGTGACCAGACA	
	R	LG-8	TGTCTGGTCACTCAC*agc*GACCTCACATGCAGA	
	F	LG-9	AAGGGTGGTTGTCAA*gct*GTTACTTGTCACCCA	
	R	LG-10	TGGGTGACAAGTAAC*agc*TTGACAACCACCCTT	

pFastbac1-GP64 -6xHis-NSvc2(F460A/ F489A/Y498A) -1xFlag	F	P4726	CCACCATCGGGCGCGGATCCatggtaagcgctattgtttt	To amplify point mutant fragment and vector fragment, then do homologous recombination to obtain plasmid
	R	P4727	aaaacaatagcgcttaccatGGATCCGCGCCCGATGGTGG	
	F	P2603	GAGGAATGGAAATGT*gct*GAAGGGGAAGGTTGC	
	R	P2604	GCAACCTTCCCCTTC*agc*ACATTTCCATTCCTC	
	F	P2605	TATTGTGTCACTGAT*gcc*CACATATTTTCCTAT	
	R	P2606	ATAGGAAAATATGTG*ggc*ATCAGTGACACAATA	
	F	P2613	TCCTATTGCCCAGCA*gcc*CACTACAATTGGAAG	
	R	P2614	CTTCCAATTGTAGTG*ggc*TGCTGGGCAATAGGA	

The terminal fusion sequences in the homologous recombination primers are in uppercase and lowercase letters; the restriction enzyme sites are the lowercase letters; the 1xFlag sequence is the italic letters; the gene sequences are underlined, and the point mutation sites are the lowercase italic letters.